American Mineralogist, Volume 75, pages 71–88, 1990

Cordierite volatile content and the role of CO_2 in high-grade metamorphism

Julie K. Vry, Philip E. Brown, John W. Valley
Department of Geology and Geophysics, University of Wisconsin, Madison, Wisconsin 53706, U.S.A.

Abstract

The channel H_2O, CO_2, and alkali contents of 33 natural cordierites have been analyzed using a combination of Fourier-transform infrared spectroscopy (FTIR), electron-microprobe analysis, and chemical and isotopic techniques. H_2O and CO_2 were analyzed by infrared spectroscopy (IR); hydrocarbons such as methane were not detected. In the IR spectra, type-II water and total (Na + K + Ca) are strongly correlated and show a 2:1 ratio. Most cordierites from granulite-facies samples are characterized by low total volatile contents, low total water, low alkalis, and high but variable X_{CO_2}($X^{crd}_{CO_2} \geq 0.3$).

If a fluid phase exists during high-grade metamorphism, then the volatiles in cordierite potentially provide useful information about metamorphic-fluid conditions. Isopleths for estimating the equilibrium amounts of total volatiles in cordierite as a function of *P*, *T*, and $X^{crd}_{CO_2}$ have been derived using published experimental data. Many natural cordierites appear relatively volatile deficient by comparison. The degree of volatile deficiency correlates to the amounts of the channel cations (Na + K + Ca) and CO_2 and most likely results from postmetamorphic leakage. Such postmetamorphic volatile losses can significantly impact the applicability of using cordierite for geobarometric studies and must also be considered in any estimation of metamorphic-fluid compositions from $X^{crd}_{CO_2}$. If volatile losses affect both H_2O and CO_2 equally, then estimates of granulite-facies fluid compositions generally indicate $X^{fluid}_{CO_2}$ values of >0.7. These $X^{fluid}_{CO_2}$ estimates could be too high by 0.15 or more if H_2O is preferentially lost during retrogression. Such estimates of $X^{fluid}_{CO_2}$ from volatile contents of cordierite do not, however, reliably reflect fluid saturation or quantities of fluid.

The C-isotope evidence for cordierites from a number of granulite-facies terranes is not consistent with theories that propose large amounts of CO_2 infiltration, and for this reason the cordierite data, taken together, are best explained by processes of dehydration by partial melting.

Introduction

Cordierite is a common metamorphic mineral in medium- and high-grade aluminous rocks. It is of petrologic interest because it participates in a number of reactions sensitive to pressure and temperature and also because the large, ring-shaped structural channels typically contain molecular H_2O, CO_2, and other species that potentially monitor metamorphic-fluid compositions. Numerous attempts have been made to calibrate cordierite geobarometers and water-fugacity indicators (summarized in Lonker, 1981; Bhattacharya, 1986; and Deer et al., 1986), and experimental methods have been used to examine and quantify the partitioning of H_2O and CO_2 between cordierite and a coexisting fluid phase (Johannes and Schreyer, 1981). However, the lack of information on the volatile compositions of natural cordierites has hindered studies of cordierite-bearing metamorphic rocks. To interpret the metamorphic assemblages and especially to attempt to draw inferences about prevailing metamorphic-fluid compositions in amphibolite- and granulite-facies rocks require a better understanding of cordierite-channel occupancy.

We have used methods of infrared (IR) spectroscopy to evaluate the amounts and proportions of channel H_2O and CO_2, and to search for other species such as methane, in 33 natural cordierites from a variety of metamorphic environments. Data obtained from these natural samples have been compared to the results of previous experiments at high pressures and temperatures and correlated to the cordierite chemical compositions, C-isotope values, and metamorphic grade. The samples analyzed include 22 cordierites from seven different granulite or transitional amphibolite-granulite terranes.

Background

Crystal chemistry

Cordierite has a simplified formula $(Mg,Fe)_2Al_4Si_5O_{18}\cdot[H_2O,CO_2]$. The crystal-chemical formula of low cordierite can be written as $(M)_2(T_11)_2(T_26)_2(T_23)_2(T_21)_2(T_16)O_{18}$, (Ch0,Ch¼), where six-membered rings of T_2 tetrahedra

0003–004X/90/0102–0071$02.00

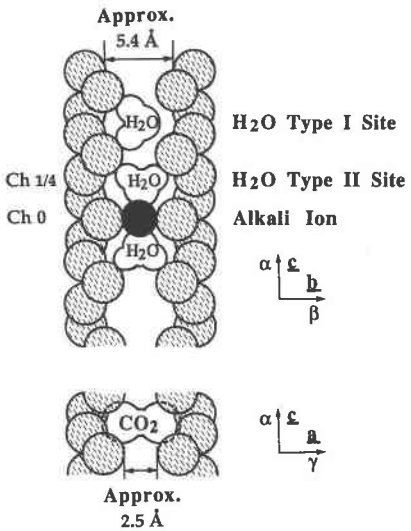

Fig. 1. Schematic representation of the cordierite crystal structure, showing orientations of channel H_2O, CO_2, and alkali cations. After Wood and Nassau (1967) and Aines and Rossman (1984).

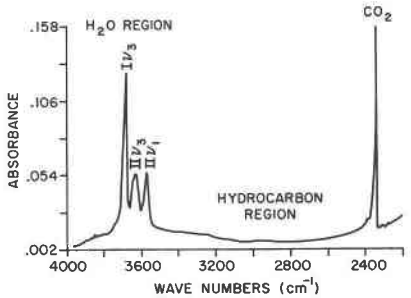

Fig. 2. Infrared spectra of cordierite powder. Asymmetric stretching (ν_3) of type-I water results in a peak near 3689 cm^{-1}, peaks from asymmetric stretching (ν_3) and symmetric stretching (ν_1) of type-II water occur near 3632 cm^{-1} and 3574 cm^{-1}, and CO_2 is resolved near 2349 cm^{-1}. Hydrocarbons such as methane will be resolved in the C-H stretching region, near 2900 cm^{-1}, but are not seen in this sample. Peak assignments after Aines and Rossman (1984).

are cross-linked into a framework by T_1 tetrahedra, Al is ordered on $T_1$1 and $T_2$6, and the octahedral M sites typically contain Mg^{2+}, Fe^{2+}, and Mn^{2+} (Gibbs, 1966; Meagher, 1967; Cohen et al., 1977; Hochella et al., 1979; Wallace and Wenk, 1980). Within the cordierite framework, ring-stacking along the *c* axis forms channels that narrow to "bottlenecks" (~2.5 Å in diameter) and widen into large "cages" with maximum dimensions of approximately 5.4 Å along *b* and 6.0 Å along *a* (Gibbs, 1966). The channel site Ch0 is in the center of a "bottleneck"; Ch¼ is a "cage" location (Fig. 1). Charge deficiency in the framework can be balanced by incorporation of additional alkali cations in Ch0, according to substitutions such as $Na^+ + Be^{2+} \rightarrow Al^{3+}$ and $Na^+ + Li^+ \rightarrow Mg^{2+}$ or Fe^{2+} (Povondra and Langer, 1971; Armbruster and Irouschek, 1983; Gordillo et al., 1985; Armbruster, 1986).

Channel volatiles

In addition to alkali cations, adsorbed molecular species such as H_2O and CO_2 commonly occur in the channels of natural cordierites (Wood and Nassau, 1967; Meagher, 1967; Povondra and Langer, 1971; Cohen et al., 1977; Hawthorne and Černý, 1977; Armbruster and Bloss, 1980, 1982; Zimmerman, 1981). Other volatile species such as He, Ar, CO, N_2, O_2, Ne, H_2S, and hydrocarbons have also been reported (Damon and Kulp, 1958; Beltrame et al., 1976; Norman et al., 1976; Mottana et al., 1983). Species such as H_2O, CO_2, and hydrocarbons produce strong infrared (IR) signals in interference-free portions of the cordierite spectrum (Fig. 2) and have been recognized and characterized by suitable methods of IR spectroscopy (Farrell and Newnham, 1967; Suknev et al., 1971; Kitsul et al., 1971; Goldman et al., 1977; Mottana et al., 1983; Aines and Rossman, 1984). In this way, certain peaks in the IR spectra (Fig. 2) have been correlated with two distinct orientations of channel H_2O molecules (Fig. 1). These orientations are designated as type I, with H-H parallel to *c*, and type II, with H-H parallel to *b* (Wood and Nassau, 1967; Goldman et al., 1977). The NMR results of Carson et al. (1982) suggest that, on the longer NMR experimental time scale (about 10^{-6} s vs. about 10^{-12} s for IR), the type-I H_2O molecule is in rapid motion between orientations with H-H parallel to *c* and H-H perpendicular to *c*. The type-II H_2O orientation is induced by the presence of cations (Na^+, K^+, Ca^{2+}, and possibly some Fe^{2+} and Fe^{3+}) in the Ch0 site (Wood and Nassau, 1967; Duncan and Johnston, 1974; Goldman et al., 1977). The large, linear CO_2 molecule aligns chiefly along *a*, within the widest channel "cage" dimension (Farmer, 1974, p. 309; Armbruster and Bloss, 1982). Space considerations indicate that a maximum of 1 mol of gas per formula unit (pfu) (2.99 wt% H_2O or 6.99 wt% CO_2 in pure Mg cordierite) can be accommodated in the channels (Johannes and Schreyer, 1981).

The contents of H_2O and of CO_2 in cordierite have been studied by both experimental techniques and, more rarely, by chemical analyses of natural samples. An extensive body of data exists for the experimental hydration of cordierite (summarized in Lonker, 1981; Schreyer, 1985; and Deer et al., 1986). The volatile equilibria involving contents of CO_2 in cordierite have been experimentally investigated by Gunter (1977), Johannes and Schreyer (1977, 1981), and Armbruster and Bloss (1982). Analytical studies of both H_2O and CO_2 in natural cordierites are few (Kitsul et al., 1971; Suknev et al., 1971; Hörmann et al., 1980; Zimmerman, 1981; Armbruster et al., 1982; Armbruster and Irouschek, 1983; Perreault and Martignole, 1986) and utilize a variety of analytical techniques. The variety of analytical methods used makes it difficult to compare the different analytical data sets or to relate volatile-composition data from natural cordierites to the results of experiments at high pressures and temperatures.

Infrared methods, if carefully calibrated, can provide analyses for specific channel-gas species (e.g., CO_2, both orientations of H_2O, and hydrocarbons). Infrared analysis requires very little sample material (~3 mg of cordierite for the KBr pellet method) and is relatively unaffected by common trace impurities such as graphite and sulfides. Micro-FTIR methods are also available and may permit future studies of volatile zonations in natural cordierites.

By contrast, it is more difficult to apply or interpret other analytical techniques used for studies of volatiles in cordierite. Optical methods (Lepezin et al., 1976; Medenbach et al., 1979, 1980; Selkregg and Bloss, 1980; Armbruster and Irouschek, 1983) can give good approximations of total gas content, but do not identify the channel-gas species. In addition, some optical methods are only applicable to Na- and Be-poor cordierites (Selkregg and Bloss, 1980; Armbruster and Irouschek, 1983). Methods involving high-temperature volatile extraction require relatively large samples (typically several hundred milligrams) and very careful mineral separation. Such large sample requirements effectively prevent the analysis of cordierites from many metamorphic rocks. Analytical errors may also be introduced by adsorbed moisture on fine-grained sample material, by pinitization in natural cordierite, and by oxidation of Fe in the cordierite itself. Many cordierite crystals also contain easily overlooked fine plates of crystallographically oriented graphite or pyrrhotite, which evolve gases upon heating. Gas analyses by absorption methods (Kitsul et al., 1971; Suknev et al., 1971) appear to give somewhat low CO_2 values compared to other methods, and the Penfield method of H_2O determination requires corrections for the presence of CO_2 and for uncondensed water.

In order to use IR methods for analyses of H_2O and CO_2 in cordierite, working curves must be developed and carefully calibrated. This approach should enable rapid H_2O and CO_2 determinations using small cordierite samples, including many that might be difficult or impossible to separate for analysis by other methods.

Experimental methods

Water and CO_2 are easily resolved in IR spectra of cordierite (Farrell and Newnham, 1967; Wood and Nassau, 1967; Goldman et al., 1977; Aines and Rossman, 1984). In IR spectra from KBr pellets of powdered cordierite (Fig. 2), CO_2 is resolved near 2349 cm^{-1}, and peaks due to asymmetric stretching (ν_3) of H_2O molecules occur at approximately 3689 cm^{-1} for type-I water (H_2O I ν_3), and 3632 cm^{-1} for type-II water (H_2O II ν_3). Symmetric stretching (ν_1) produces a peak (H_2O II ν_1) near 3574 cm^{-1}; and bending (ν_2), a peak (H_2O II ν_2) near 1630 cm^{-1}. Hydrocarbons produce strong peaks in the C-H stretching region (near 2900 cm^{-1}), but were not observed in any of the cordierite samples studied.

Good peak-height reproducibility was obtained using 13-mm diameter KBr pellets, prepared from 3 mg of finely ground cordierite and 100 mg of dry spectroscopic-grade KBr, weighed to within 0.1 mg and pressed at 10 tons ram pressure in a pellet press. The small cordierite sample size was selected in order to simplify mineral-sample preparation. Care was taken to limit moisture adsorption during weighing. The pellets had a uniform thickness of about 0.28 mm, measured for several samples using an optical microscope.

Spectra were generally obtained in the 4000 to 2200 cm^{-1} region using a Nicolet 5DX FTIR, purged with dry N_2 gas. Careful purging is necessary in order to avoid effects related to slight changes in atmospheric CO_2. The CO_2 peak positions in cordierite and the atmosphere are not appreciably shifted from one another, so minor variations in atmospheric CO_2 might otherwise be included, with potentially serious effects, in analyses of the small cordierite samples. Background effects due to H_2O in the KBr were minimal for most samples and were easily subtracted.

Quantitative chemical analyses were performed for eight major and minor elements on the ARL-SEMQ electron microprobe at the University of Wisconsin, Madison. The cordierite samples were analyzed by wavelength-dispersive methods, using well-characterized mineral standards, a defocused beam (~15–20 μm in diameter), a 15-kV accelerating potential, and a sample current of 15 nA. Count times of 15 to 20 s per spot, with a total of 8 to 10 spots analyzed per grain, were used for major elements. Energy-dispersive analyses of at least 250 s were used to check for unanalyzed elements. Minor elements were counted for a minimum of 500 s, 40 to 100 s per spot. Whenever possible, a total of 10000 X-ray counts were collected for Na, which is the most important of the channel alkali cations, requiring total count times of up to 2000 s for several samples. Volatilization checks, made for four times the counting time for Na, showed no specimen damage. Oxide weight percents were calculated using the correction procedures of Bence and Albee (1968). Minimum detection limits for Na and K, at three times the X-ray standard deviation, were 0.03 and 0.02 wt%, respectively. Both the major- and minor-element compositions showed good homogeneity over the sample areas studied. Totals approximate 100% for nearly all of the samples, supporting the view that H_2O, CO_2, and alkali cations constitute the major channel occupants. No analytical determinations for Li^+ and Be^{2+} were obtained in this study; if present, these light elements would produce only very slight increases in the estimated weight percentage totals.

Calibration curve for CO_2

The IR working curve for CO_2 (Fig. 3) was calibrated using measurements obtained during the extraction of CO_2 for C-isotope analyses (Vry et al., 1988). The CO_2 was isolated from 200 to 775 mg of pure, gemmy cordierite by grinding with excess CuO and heating at 1050 °C in a vacuum-extraction line. Hand-picking of the cordierite separates for thermal gas extraction required 5–30 h per sample, because great care was taken to avoid any traces of graphite, sulfides, or visible regions of possible alteration. The 1050 °C temperature was selected after ther-

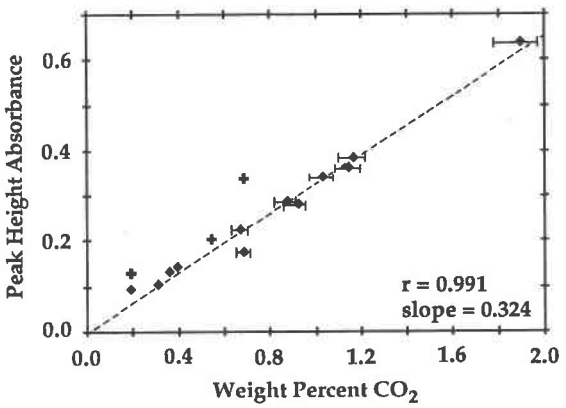

Fig. 3. IR working curve for CO_2 in cordierite (KBr pellet technique; IR peak near 2349 cm^{-1}). Manometric CO_2 determinations (solid diamonds) were obtained in this study and used in locating the working curve. IR measurements (crosses) are included for comparison purposes and show samples for which CO_2 was determined by titration (Th. Armbruster, personal communication).

mogravimetric analyses (TGA) of similar finely ground cordierite samples showed that volatile evolution begins near 450 °C and is effectively complete by 900 °C (A. B. Hunter, personal communication). These temperatures are in agreement with the results of Zimmerman (1981) and Aines and Rossman (1984), who showed that heating to 900 °C was required to expel all CO_2, and Suknev et al. (1971), who found weight losses complete by 800 °C.

The CO_2 was cryogenically purified and manometrically measured. The manometer measurements have an uncertainty of ~0.5 μmol CO_2. The minimum detection limit of this technique was determined by analysis of blanks, samples containing no cordierite, which produced less than 1 μmol of CO_2. For small cordierite samples with low CO_2 contents, 1 μmol of CO_2 corresponds to an uncertainty of about 0.02 wt% CO_2. Replicate analyses for CO_2 were obtained from separately prepared samples of five different cordierites. For each of these cordierites, measured CO_2 contents were reproducible to within ±0.04 wt% CO_2.

The KBr pellets used for calibrating the IR working curves were prepared from splits of the same cordierite separates used for isotope analyses. Because finely ground cordierite might be subject to either moisture absorption or volatile losses after grinding, the cordierite chips (usually 40 to 20 mesh, larger when possible) were not ground finely until immediately prior to sample preparation. Because some natural cordierites show marked volatile heterogeneities within large single crystals (±50%, Rossman, personal communication) and because the KBr pellets require very little sample material, it is possible to prepare pellets having volatile compositions noticeably different than the bulk analyses. For this reason, the KBr pellets used in calibrating the IR working curves were made from the large, well-mixed cordierite powder samples prepared for isotope studies.

Figure 3 clearly shows that the KBr pellet technique is effective for determining cordierite CO_2 contents, given uniform handling procedures and well-calibrated standards. The error bars reflect the weighing uncertainty of ±0.1 mg and possible losses of up to 3% of the total sample during the pressing of KBr pellets. These errors could introduce an uncertainty in the final CO_2 estimates of at most ±0.1 wt% (<0.014 mol pfu for pure-Mg cordierite) for CO_2-rich samples and ±0.07 wt% (<0.009 mol pfu) for samples with less than 0.4 wt% CO_2. For duplicate, separately weighed samples, CO_2 estimates using IR peak-height absorbance measurements were normally reproducible to within ±0.05 wt% CO_2. There was good uniformity of cordierite distribution within the KBr pellets, as examined by rotating several of the pellets within the sample holder and collecting additional, replicate spectra, with excellent reproducibility of analyses.

The close fit (Fig. 3) of the IR peak-height absorbance data to CO_2 content measurements by thermal extraction reflects both the extreme care expended in preparation of the large samples for volatile extraction and the careful purging of the IR sample chamber prior to analysis. The linearity of the working curve permits estimation of a wide range of cordierite CO_2 compositions by using only a few calibration standards.

It would be desirable to separate large samples of homogeneous cordierite that could be used as calibration standards by many laboratories; however, most cordierite samples are either small or possibly heterogeneous in volatile content. Of the cordierites studied, samples 21–23 are well analyzed, exceptionally clean, and appear to be fairly uniform and similar in volatile composition. However, these cordierite specimens are not large. Very large quantities of sample 25 are available, but the volatile-content uniformity has not been evaluated. Only very limited amounts of samples 6, 13, and 15 exist, and for this reason these samples are much less suitable for use as calibration standards. The cordierite from White Well, Australia (sample 27), has been studied by many workers and may provide a useful standard if the volatile content is not variable.

The CO_2 data obtained in this study compare fairly well to previous data obtained by other analytical methods. Th. Armbruster supplied us with three well-studied cordierite specimens that had previously been analyzed by coulometric titration (Johannes and Schreyer, 1981). Our IR analyses of these samples indicate somewhat higher CO_2 contents than the titration results (approximately 0.1 to 0.3 wt%, or 0.014 to 0.042 mol CO_2 pfu; see Fig. 3). It is not known whether these results reflect differences in cordierite sample preparation, differing analytical sensitivities for the two methods, or real differences in a slightly heterogeneous sample. However, the excellent self-consistency of the data obtained in this study suggests that the analyses are both accurate and precise (Fig. 3).

Calibration curve for water

The IR working curve for H_2O (Fig. 4) was calibrated by using two hydrogen-manometer measurements ob-

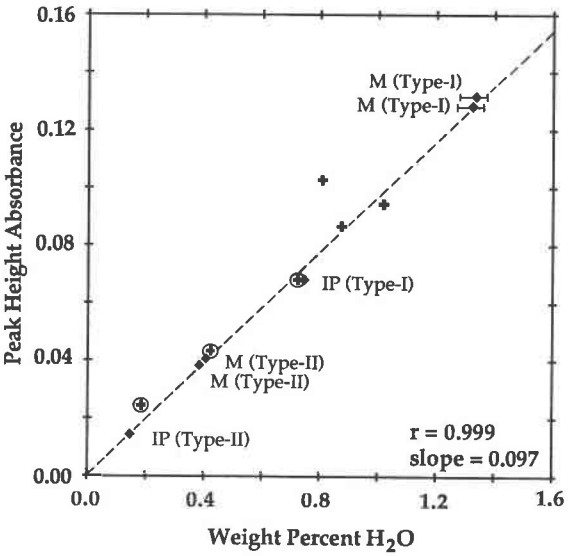

Fig. 4. IR working curve for H_2O in cordierite (KBr pellet technique; IR peak height measurements near 3689 cm^{-1} and 3632 cm^{-1} for type-I and type-II H_2O, respectively). Diamonds indicate samples from this study used in locating the working curve: total H_2O contents determined by manometer (M) after high-temperature gas extraction and by ion microprobe (IP). Additional IR measurements, included for comparison purposes, for samples in which total H_2O was determined by titration (Th. Armbruster, personal communication): crosses indicate type I, and crosses within circles indicate type II. The molar absorptivity coefficients for type I and type II H_2O were assumed to be equal.

tained during H-isotope analyses run by S. R. Dunn, in James R. O'Neil's laboratory at the U.S. Geological Survey in Menlo Park, and an ion-microprobe analysis by Richard L. Hervig at Arizona State University. The hydrogen-manometer measurements were reproducible to within ±0.02 wt%. In the application of this technique, it proved critically important to dry the cordierite samples at least overnight under a hard vacuum at temperatures above 100 °C, in order to remove adsorbed moisture. Four replicate H_2O determinations by ion microprobe gave values of 1.1, 0.9, 0.8, and 0.8 wt% (av. 0.9 wt%). The error bars shown in Figure 4 reflect the same weighing and sample-transfer uncertainties discussed above for the CO_2 working curve. For samples containing small amounts of H_2O, these errors become progressively less, to the effect that error bars could be represented for only two of the points shown in Figure 4. The spectra used in developing this working curve show very nearly flat baselines in the H_2O stretching region (Fig. 2), minimizing uncertainties in the peak-height absorbance measurement.

The molar absorptivity coefficients for type-I and type-II water molecules (asymmetric stretching, H_2O I ν_3 and H_2O II ν_3) were assumed to be equal. This assumption is consistent with the results of Goldman et al. (1977, p. 1154) and also provides data consistent with a model involving the coordination of two type-II H_2O molecules to each alkali cation (Fig. 6, discussed in a later section). It is quite possible that the molar absorptivity coefficient

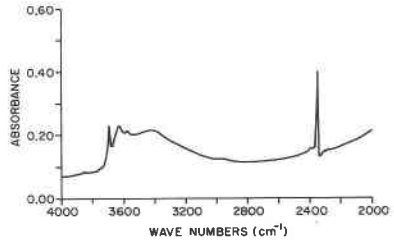

Fig. 5. Example of uneven IR spectral baseline in the H_2O stretch region (near 3500 cm^{-1}), seen only in samples 24 and 31. Spectrum is of sample 24.

for type-II H_2O is slightly less than that for type-I H_2O, as was reported by Goldman et al. (1977). If true, this would introduce only very small changes in the estimated proportions of type-I and type-II H_2O and would not change the values reported for total H_2O contents. The measured ratio of type-II H_2O to alkali cations is close to 2:1 and thus is a strong indication that the stated assumption is valid.

H_2O baseline

During the course of this study, two samples were encountered (Manitouwadge, Ontario, no. 24; Kragero, Norway, no. 31) that showed unusual baseline effects in the water region of the IR spectrum. Although these two samples appeared visually clean and virtually unaltered, the IR spectra show a pronounced, diffuse water peak, such as might be expected from adsorbed moisture in the KBr pellet or from water in fluid inclusions (Fig. 5, compare to Fig. 2). New KBr sample pellets were prepared after redrying the cleaned, coarsely broken sample grains 2.5 d at 120 °C. The spectra obtained from these new pellets did not differ appreciably; the baselines were still markedly uneven. These two samples yielded consistently high backgrounds even though other samples prepared at the same time, from the same KBr, provided spectra with nearly flat baselines, as in Figure 2.

Although IR estimates of the weight percentage of (type-I + type-II) water can be measured above the curving baseline for these two samples, and compare well with previous titration analyses, the values obtained are not consistent with the measured alkali contents (Fig. 6, discussed in following section). Type-II water estimates for these two anomalous samples, when checked against electron-microprobe analyses for alkali cations (Fig. 6) were consistently far higher than would be predicted from the assumption, based on all of our other analyses and on the work of Goldman et al. (1977), that two type-II H_2O molecules are associated with each alkali cation (Fig. 1). We are unable to determine the cause of these unusual baseline effects; however, the fact that these effects were observed in only two samples of all those studied suggests that the samples are atypical. Cordierite specimens displaying this broad water peak in the IR spectra may not be appropriate for studies of H_2O content using the KBr pellet technique.

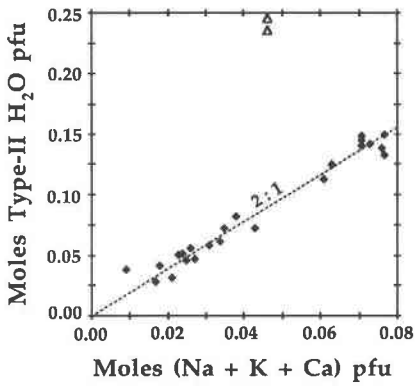

Fig. 6. Correlation of two type-II H_2O molecules with each channel cation (Na, K, Ca). Dashed line shows 2:1 ratio. Solid diamonds indicate cordierite samples with normal IR baselines. When compared to measured alkali contents, the two cordierite samples (24 and 31, indicated by open triangles) that display uneven IR baselines in the H_2O stretching region give anomalously high IR H_2O estimates.

For all samples (except nos. 24, 31), our final working curve for H_2O (Fig. 4) provided water estimates remarkably consistent with alkali-cation analyses (Fig. 6) and in close agreement with previous titration analyses. This should permit comparisons of the natural-sample data to the results of previous optical and high-pressure experimental studies, where H_2O and CO_2 have either been separately analyzed by coulometric titration (described in Johannes and Schreyer, 1981), or total gas contents have been determined by optical methods (described in Lepezin et al., 1976; Medenbach et al., 1979, 1980; Selkregg and Bloss, 1980; Armbruster and Irouschek, 1983).

Results

Sample descriptions are given in Table 1, analyses of H_2O and CO_2 by IR and other methods are summarized in Table 2, and electron-microprobe analyses for selected cordierite samples are given in Table 3.

From the data obtained in this study, the ratio of absorptivity coefficients for CO_2/H_2O is estimated to be approximately

$$a_{CO_2}/a_{H_2O\ I\ \nu_3\ or\ II\ \nu_3} \approx 3.34$$

on a weight percent basis, or

$$\epsilon_{CO_2}/\epsilon_{H_2O\ I\ \nu_3\ or\ II\ \nu_3} \approx 8.16$$

on a molar basis, where a and ϵ are absorptivity coefficients. For a uniform distribution of cordierite in the KBr pellet, this gives

$$\epsilon_{CO_2} \approx 630\ \text{L}\cdot\text{mol}^{-1}\cdot\text{cm}^{-1},$$

and

$$\epsilon_{H_2O\ I\ \nu_3\ or\ II\ \nu_3} \approx 77\ \text{L}\cdot\text{mol}^{-1}\cdot\text{cm}^{-1}.$$

These values are based upon Beer's law for both CO_2 and H_2O and upon the stated assumption that absorptivity coefficients for type-I and type-II H_2O are approximately equal. Beer's law can be expressed as $A = \epsilon bc$, where A is the measured absorbance, b is the path length in centimeters, c is concentration, and ϵ is an absorptivity coefficient with units of $\text{L}\cdot\text{mol}^{-1}\cdot\text{cm}^{-1}$. If concentration is to be described in other units, such as weight percent, then the absorptivity coefficient is usually represented by the symbol a.

The above values are in marked contrast to the molar absorptivity coefficients for powdered cordierite samples cited in Aines and Rossman (1984), which are

$$\epsilon_{CO_2} = 6000 \pm 500\ (\text{L}\cdot\text{mol}^{-1}\cdot\text{cm}^{-1})$$

and

$$\epsilon_{H_2O\ I\ \nu_3} = 210 \pm 10\ (\text{L}\cdot\text{mol}^{-1}\cdot\text{cm}^{-1}) \approx \epsilon_{H_2O\ II\ \nu_3},$$

giving a ratio of

$$(\epsilon_{CO_2})/(\epsilon_{H_2O\ I\ \nu_3\ or\ II\ \nu_3}) \approx 28.6$$

for the same peak locations. The discrepancy probably results largely from the previous authors' selection of molar absorptivity coefficients for "water" (Goldman et al., 1977, p. 1151) that represented total gas contents, without consideration of CO_2.

Relationship of type-II H_2O to total alkali contents

On the basis of optical absorption, Mössbauer, and X-ray studies, Goldman et al. (1977) suggested that the presence of certain ions (Na^+, Ca^{2+}, or minor Fe^{3+} or Fe^{2+}) in the channel bottleneck site, Ch0, induces the type-II orientation in immediately adjacent Ch¼ H_2O molecules. From their data they inferred that other cations, capable of producing similar orientation effects, also occupied the channels. Our analyses suggest that K can also be an important channel constituent, although it is rarely present in more than trace amounts. The excellent fit of our type-II H_2O data to alkali-cation (Na + Ca + K) contents (Fig. 6) argues against the importance of other cations in the channels of the cordierites we have studied.

Figure 6 shows the relationship of type-II H_2O estimates to (Na + Ca + K) contents. The 2:1 ratio predicted by Goldman et al. (1977) is clear. These data give an added indication of the high precision obtainable in routine estimates of the H_2O content of cordierite channels by using the KBr pellet method. This good agreement strongly suggests that type-II H_2O can be accurately estimated (to better than ±0.06 wt%, or 0.02 mol pfu) even for the small, 3-mg samples used in this study. The precision of both water and CO_2 analyses is thus similar, despite the marked differences in observed peak heights that result from the differing molar absorptivity coefficients.

Characteristics of granulite-facies cordierites

In comparison to cordierites collected from other occurrences, most cordierites from the granulite facies are characterized by a combination of low contents of total volatiles, high but variable $X^{crd}_{CO_2}$ (generally $X^{crd}_{CO_2} = 0.3$ to 0.7), and extremely low contents of channel alkalis [(Na

TABLE 1. Cordierite sample information

Sample no. in this paper	Identifier	Locality (lateral distance to opx isograd, if known)	Local conditions and/or facies (references)*	Minerals (references)*	Source**
1	CL-177-1	Pikwitonei granulite domain (PGD), Manitoba, Canada; N. Cauchon Lake (7.5 km)	648 °C, 6.1–6.8 kbar; granulite (AA)	Qtz(rt), pl, kfs, bt, crd, gr, ilm, po, [py], spl, zrn	A
2	M218	PGD, N. Cauchon Lake; same outcrop as 177-1	648 °C, 6.1–6.8 kbar; granulite (AA)	Pl, kfs, bt, crd, gr, grt, rt, ilm	B
3	CL-97-2	PGD, N. Cauchon Lake (7–7.5 km)	774 °C, 6.1–6.8 kbar; granulite (AA)	Qtz(rt), kfs, bt, crd, opx, grt, po, zrn	A
4	CL-97-7A	PGD, N. Cauchon Lake; same outcrop as 97-2	774 °C, 6.1–6.8 kbar; granulite (AA)	Qtz, kfs, bt, crd, grt, [py], [ccp], zrn	A
5	CL-100-10	PGD, N. Cauchon Lake (7–7.5 km)	648 °C, 6.1–6.8 kbar; granulite (AA)	Qtz, pl, kfs, bt, crd, gr, grt, spl, ilm, rt, zrn	A
6	CL-231-4	PGD, Prud'homme Lake (9 km)	750 °C, 6.1–6.8 kbar; granulite (AA)	Crd, bt, rt, po, zrn	A
7	M346	PGD, Prud'homme Lake (9 km)	780 °C, 6.4 kbar; granulite (AA)	Qtz, kfs, bt, grt, crd, gr	B
8	M401	PGD, S. Cauchon Lake (0.5 km)	640 °C, 6.1–6.8 kbar; granulite (AA)	Pl, kfs, bt, crd, gr, grt, sil	B
9	NL-419-1	PGD, Natawahunan Lake (~47 km)	770–800 °C, 6.9–7.8 kbar; granulite (AA) (generally clean, but retrograde hydration evident in most rock types, this locality)	Qtz, pl, kfs, bt, crd, grt, sil, ilm, rt, spl	A
10	Bamble 3	Bamble region, Norway	Amphibolite-granulite transition	Pl, bt, crd, grt, amph	C
11	84TV-24	Bamble region, Norway; Risör district	Amphibolite-granulite transition	Qtz, pl, bt, crd, grt, rt, ilm, po	C
12	12348	Arendal, Norway	800 °C, ~9 kbar; granulite (BB)	Bt, crd, grt, amph	M
13	Grizzley Creek	Laramie Range, Wyoming	<600 °C, ~4 kbar; amphibolite (CC)	Ky, crd, cm, (±sil, ±ged, ±mrg, ±st) (CC)	D
14	Crescent Lake	Wind River Range, Wyoming	>750 °C, 5 kbar; granulite (CC)	Bt, kfs, grt, opx (CC)	D
15	135.489	Manivitsy, Madagascar	Granulite (DD)	Krn, bt, crd, sil, crn, spl, and, grd (DD)	G, H
16	NE86A-24A	Sturbridge, Massachusetts	675–730 °C, 6.3 kbar; granulite (EE)	Qtz, pl, kfs, bt, crd, grt, gr, sil, rt, zrn, opaques	I
17	NE86A-24B	Sturbridge, Massachusetts	675–730 °C, 6.3 kbar; granulite (EE)	Qtz, pl, kfs, bt, crd, grt, sil, opaques	I
18	NHQ-1	Nelson House quarry, Nelson House, Manitoba	amphibolite	Qtz, kfs, bt, crd, gr, grt	A
19	Brazil	Minas Gerais, Gouvernardor Valadareao, Brazil		Qtz, pl, bt, chl, crd, gr, grt, amph, ilm, rt, spl, [s]	J
20	S. India 1	Kerala, South India, Khondalite belt	750 °C, 5–6 kbar; amphibolite-granulite transition (FF)	Pl, crd, grt, sil, spl (FF)	L
21	3083E	Ellammankovilpatti, Tamil Nadu, India	750 °C, 5–6 kbar; granulite (GG)	Krn, sil, hgb, crd, spl, mag, rt (GG)	G
22	3083D	Ellammankovilpatti, Tamil Nadu, India	750 °C, 5–6 kbar; granulite (GG)	Krn, sil, crd, rt, zrn, mnz (GG)	G
23	3083D1	Ellammankovilpatti, Tamil Nadu, India	750 °C, 5–6 kbar; granulite (GG)	Krn, sil, crd, rt, zrn, mnz	G
24	Manitouwadge	Manitouwadge, Ontario, Canada	Amphibolite	Crd, ccp, py, qtz, bt, felds, grt	J
25	GECO	GECO mine, Manitouwadge, Ontario, Canada	Amphibolite	Crd, po, ccp, py, qtz, bt, felds	K
26	Tanzania gem	Tanzania		Crd	M
27	White Well	White Well, Western Australia		Crd, crn, phl, drv, sil, zrn, rt (HH)	M
28	Hards Range	Australia		Crd	M
29	Great Bear Lake	Great Bear Lake, N.W. Territories, Canada		Crd	J
30	WYO-1	Albany County, Wyoming	Metasomatic? (II)	Crd	E, F
31	Kragero	Kragero, Norway	Amphibolite	Crd	M
32	WYO-2	Albany County, Wyoming	Metasomatic? (II)	Crd	F
33	171.350	Southern Madagascar	Granulite	Crd, opx, krn (JJ)	G, H

Note: Mineral abbreviations: amphibole (amph), andalusite (and), apatite (ap), biotite (bt), chalcopyrite (ccp), chlorite (chl), cordierite (crd), corundum (crn), dravite (drv), feldspar (felds), garnet (grt), gedrite (ged), grandidierite (grd), graphite (gr), högbomite (hbg), ilmenite (ilm), K-feldspar (kfs), kornerupine (krn), kyanite (ky), magnetite (mag), margarite (mrg), monazite (mnz), orthopyroxene (opx), phlogopite (phl), plagioclase (pl), pyrite (py), pyrrhotite (po), quartz (qtz), rutilated quartz [qtz(rt)], rutile (rt), sillimanite (sil), spinel (spl), staurolite (st), sulfur (s), zircon (zrn). Square brackets indicate probable secondary minerals.

* References: (**AA**) Mezger et al. (unpublished manuscript); (**BB**) Peterson and Valley (1988); (**CC**) R. Frost, personal communication; (**DD**) Grew (1986); (**EE**) Robinson et al. (1986); (**FF**) Chacko et al. (1987); (**GG**) Grew et al. (1987); (**HH**) Pryce (1973); (**II**) Iiyama (1960); (**JJ**) E. Grew, personal communication.

** Sample sources: (**A**) J. Vry; (**B**) K. Mezger; (**C**) J. W. Valley; (**D**) R. Frost; (**E**) M. Cosca; (**F**) Cureton Mineral Co., Tucson, Arizona; (**G**) E. Grew; (**H**) Musée Nationale d'Histoire Naturelle, Paris, France; (**I**) D. Moecher; (**J**) D. Perkins; (**K**) P. E. Brown; (**L**) T. Chacko; (**M**) Th. Armbruster.

TABLE 2. Estimated channel-gas compositions and $\delta^{13}C$ values for natural cordierites

Sample	$\delta^{13}C_{crd}$ permil ($\delta^{13}C_{gr}$)*	Wt% CO_2	Wt% total H_2O	Wt% type-I H_2O	Wt% type-II H_2O	Moles CO_2 pfu**	Moles H_2O I pfu**	Moles H_2O II pfu**	Total moles (H_2O + CO_2) pfu**	X_{CO_2}** in cordierite
1	−34.9	1.11†	0.86	0.74	0.12	0.155	0.251	0.041	0.447	0.347
	(−41.8)	1.15‡								
2	−33.4	0.91‡								
	(−40.0)									
3	−11.2	1.97†	0.59	0.47	0.12	(0.27)	(0.16)	(0.04)	(0.47)	(0.57)
		1.90‡								
4	−14.9	1.58†	0.60	0.60	b.d.	(0.22)	(0.20)	b.d.	(0.42)	(0.52)
5		0.98†	0.74	0.60	0.14	(0.13)	(0.19)	(0.05)	(0.37)	(0.35)
6	−11.0	1.18†	0.85	0.70	0.15	0.163	0.236	0.051	0.450	0.362
		1.17‡	0.9‖							
7	−31.8	1.52†	0.33	0.27	0.06	(0.21)	(0.09)	(0.02)	(0.32)	(0.65)
	(−36.1)									
8	−32.9	0.88†	0.72	0.64	0.08	0.123	0.218	0.027	0.368	0.334
	(−40.6)									
9		0.65†	0.88	0.60	0.28	(0.09)	(0.20)	(0.09)	(0.38)	(0.24)
10	−10.0	1.05†	0.87	0.69	0.18	0.145	0.233	0.061	0.439	0.330
		1.04‡								
11		1.16†	0.96	0.75	0.21	0.162	0.257	0.072	0.491	0.330
12		1.61†	1.04	0.83	0.21	0.226	0.285	0.072	0.583	0.388
13	−12.7	0.89†	1.05	0.68	0.37	0.122	0.228	0.124	0.474	0.257
		0.88‡								
14		1.67†	0.58	0.47	0.11	0.232	0.159	0.037	0.428	0.542
15	−6.9	1.31†	0.60	0.51	0.09	0.182	0.173	0.031	0.386	0.472
16§	−21.8	1.07†	0.57	0.44	0.13	0.155	0.156	0.046	0.357	0.434
	(−25.1)	1.28‡								
17		1.37†	0.56	0.43	0.13	0.194	0.149	0.045	0.388	0.500
18	−21.7	0.68†	0.61	0.45	0.16	0.096	0.156	0.055	0.307	0.313
	(−25.8)	0.68‡								
19	−7.4	0.53†	0.93	0.50	0.43	0.075	0.172	0.148	0.395	0.190
	(−10.5)	0.69‡								
20	−20.8	0.88†	0.56	0.40	0.16	0.125	0.139	0.055	0.319	0.392
		0.93‡								
21	−18.5	0.32†	1.79	1.35	0.44	0.039	0.458	0.149	0.646	0.060
		0.20‡								
22		0.37†	1.73§§	1.34	0.39	0.049	0.454	0.132	0.635	0.077
23	−20.5	0.31†	1.74§§	1.33	0.41	0.043	0.449	0.138	0.630	0.068
		0.32‡								
24		0.82†	1.45††	0.91††	0.54††	0.116	0.364	0.236	0.716	0.162††
25	−15.1	0.44†	1.17	0.84	0.33	0.061	0.284	0.112	0.457	0.133
		0.40‡								
26		1.29†	1.50	1.09	0.41	0.181	0.374	0.141	0.696	0.260
27		0.62†	1.29	1.05	0.24	0.085	0.353	0.081	0.519	0.164
		0.55‡‡	1.0‡‡							
28		1.04†	1.32	0.88	0.44	0.143	0.295	0.144	0.582	0.246
		0.69‡‡	1.31‡‡							
29		0.69†	1.24	1.08	0.16	0.098	0.374	0.057	0.529	0.185
30	−14.6	0.41†	0.92	0.66	0.26	(0.06)	(0.22)	(0.09)	(0.37)	(0.16)
		0.37‡								
31		0.40†	1.75††	1.02††	0.73††	0.055	0.344	0.246	0.645	0.085††
		0.20‡‡	1.75‡‡							
32		1.31†	1.47	1.06	0.41	0.182	0.360	0.140	0.682	0.267
33		1.49†	0.74	0.59	0.15	0.200	0.195	0.050	0.445	0.449

Note: b.d. = below detection limits.

* Coexisting graphite analyzed from same rock sample.

** Parentheses indicate samples for which microprobe analyses were not performed. Molar compositions for these samples were estimated by assuming a formula weight for dry cordierite of 595 g, corresponding to X_{Mg} = Mg/(Mg + Fe) = 0.84.

† CO_2 and both types of H_2O estimated from IR working curves (this study).

‡ CO_2 measured by manometer (this study).

‖ Total H_2O determination by ion microprobe (R. Hervig, personal communication).

§ Probable graphite in cordierite sample.

§§ Total H_2O determination by hydrogen manometer (S. Dunn, personal communication).

†† Uneven IR spectral baseline in H_2O stretching region; IR H_2O estimates uncertain.

‡‡ CO_2 and total H_2O determinations by separate coulometric titrations (Th. Armbruster, personal communication).

+ K + Ca) ≤ 0.05 mol pfu] (Figs. 7 and 8). The high $X^{crd}_{CO_2}$ values result largely from low total H_2O (≤0.35 mol pfu); absolute CO_2 contents are variable and in many cases are not especially high (Fig. 8). One unusual occurrence of water and alkali-rich cordierite was found, apparently of granulite-facies origin (samples 21–23, see Figs. 7 and 8). Such samples may reflect unusual local fluid environments or late high-temperature re-equilibration with H_2O-

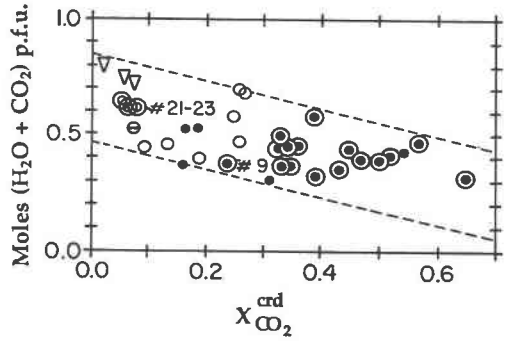

Fig. 7. Channel constituent compositions of natural cordierites. Circles around other symbols indicate samples from granulite-facies, or transitional granulite-facies, localities. Channel alkali contents (Na + K + Ca) are shown by the following symbols: solid dots indicate (Na + K + Ca) ≤ 0.05 mol pfu; small open circles, 0.05 < (Na + K + Ca) ≤ 0.10 mol pfu; small circle with crossbar, 0.10 < (Na + K + Ca) ≤ 0.15 mol pfu; and inverted open triangles, (Na + K + Ca) > 0.20 mol pfu. Cordierite in sample 9 is probably a retrograde phase, and samples 21–23 are from an unusual kornerupine-bearing assemblage. Data for five alkali-rich cordierites are from Armbruster and Irouschek (1983).

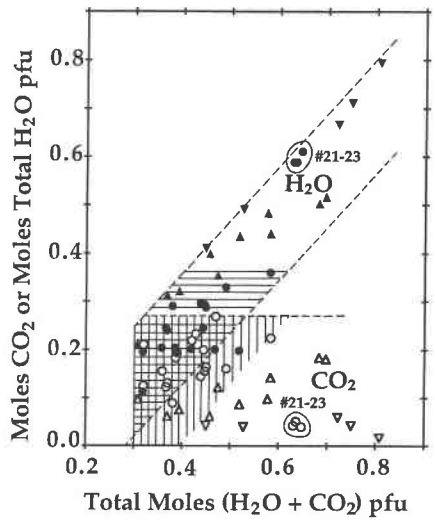

Fig. 8. Volatile compositions of natural cordierites. Circles show cordierites from granulite-facies and transitional granulite-facies occurrences, triangles represent other cordierite samples (this study), and inverted triangles represent alkali-rich cordierites (Armbruster and Irouschek, 1983). Open symbols indicate CO_2; filled symbols indicate H_2O.

rich fluids, as discussed by Grew et al. (1987, p. 27) for samples 21–23, which are from kornerupine- and hoegbomite-bearing rocks in south India.

Previous experiments

H_2O

The incorporation of H_2O into cordierite has been experimentally studied at high pressures and temperatures. Figure 9 shows the results of several experimental hydration studies at 600 °C (Schreyer and Yoder, 1964; Mirwald and Schreyer, 1977; Mirwald et al., 1979; Armbruster and Bloss, 1980; Schreyer, 1985), as well as the calculated values of Helgeson et al. (1978). For conditions corresponding to high-grade regional metamorphism, these hydration results differ significantly, but can be grouped into two sets. The results of Mirwald and Schreyer (1977) and Armbruster and Bloss (1980) are very similar and show somewhat higher total H_2O contents (about 0.1 mol pfu higher at 600 °C and 5 kbar) than the results of Schreyer and Yoder (1964), Helgeson et al. (1978), and Mirwald et al. (1979). The recent experiments reported by Schreyer (1985) do not extend to pressures above about 4 kbar and show somewhat lower H_2O contents than previous studies.

Isopleths indicating total H_2O contents as a function of pressure and temperature are plotted in Figures 10a and 10b. At conditions corresponding to high-grade regional metamorphism, the data of Mirwald and Schreyer (1977) and Armbruster and Bloss (1980) (Fig. 10a) have lower slopes and generally higher values than the results obtained by Helgeson et al. (1978) and Mirwald et al. (1979) (Fig. 10b).

H_2O-CO_2

The incorporation of CO_2 into channel-evacuated Mg-rich cordierite from White Well, Australia, has been experimentally studied by Armbruster and Bloss (1980, 1982). They showed that the equilibrium CO_2 content of this cordierite is 2.61 wt% CO_2 (about 0.36 mol pfu) at 5 kbar and 600 °C.

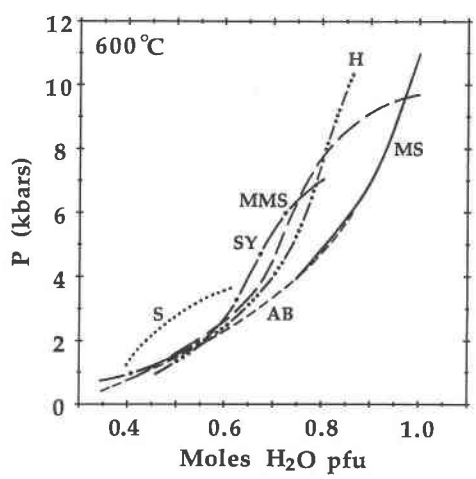

Fig. 9. Experimental studies of H_2O in cordierite, at 600 °C. Sources of experimental results: SY, Schreyer and Yoder (1964; dashes with dots); MS, Mirwald and Schreyer (1977; solid line); MMS, Mirwald et al. (1979; long dashes); AB, Armbruster and Bloss (1980; short dashes); and S, Schreyer (1985; dotted line). Values calculated by Helgeson et al. (1978) are indicated by H (dashed line with triple dots).

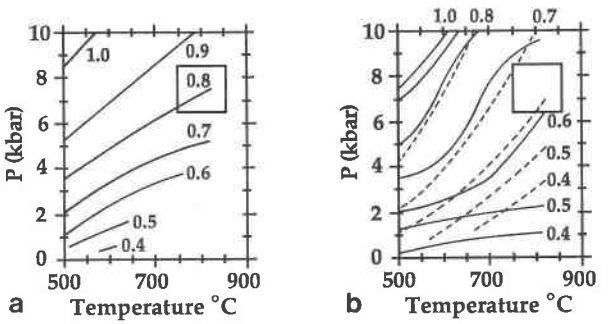

Fig. 10. Isopleths for total H_2O (in moles pfu) in cordierite at $X^{vol}_{CO_2} = 0$. (**a**) Experimental results of Mirwald and Schreyer (1977) and Armbruster and Bloss (1980). (**b**) Steeper isopleths obtained experimentally by Mirwald et al. (1979) (solid lines) and isopleths calculated by Helgeson et al. (1978) (dashed lines). Boxes show commonly reported *P-T* conditions of granulite-facies metamorphism.

The mixed-volatile partitioning of H_2O and CO_2 into synthetic pure-Mg cordierite was studied by Johannes and Schreyer (1981). They found that for a wide range of fluid compositions, cordierite preferentially incorporates H_2O in comparison to CO_2. They also reported that the choice of synthetic starting materials had a profound influence upon their experimental results. Therefore, two different sets of diagrams, for synthetic cordierites A and B, were presented, showing the partitioning of H_2O and CO_2 between cordierite and a coexisting fluid phase.

Applications to high-grade metamorphic-fluid studies

The data obtained from our natural samples (Tables 1 and 2), as well as other data from the literature (e.g., Armbruster et al., 1982; Armbruster and Irouschek, 1983) appear broadly consistent with the experimental results discussed above. By studying the natural samples, however, it becomes possible to examine several long-standing questions: (1) Which of the mixed H_2O-CO_2 partitioning experiments, if any, provide results comparable to the volatile compositions observed in natural cordierite? (2) How will isopleths for mixed H_2O-CO_2 volatile contents in cordierite differ, in general, from those determined using H_2O alone? (3) Which natural cordierites will be least subject to retrograde volatile losses, and what is the probable magnitude of volatile losses at various volatile and alkali compositions? And (4) to what extent can the H_2O-CO_2 compositions of cordierite be used as evidence of metamorphic-fluid conditions?

Experiments

In order to obtain reliable estimates of metamorphic-fluid conditions, it is necessary to have appropriate experimental data. The markedly different experimental results obtained for H_2O-CO_2 in two cordierite samples, A and B (Johannes and Schreyer, 1981), have, as a result, tended to limit the applicability of cordierite for high-grade metamorphic-fluid studies. Maximum CO_2 contents reported for cordierite B at 600 °C and 5 kbar were on the order of 1.0 wt% (~0.13 mol pfu) at $X^{fluid}_{CO_2} = 1.0$; this

Table 3. Electron-microprobe analyses (wt% oxides) of selected cordierite samples

	1	6	8	10	11	12	13	14	15	16*	17	18	19
SiO_2	48.40	49.40	48.70	49.00	48.49	48.47	48.66	48.80	48.56	46.66	47.99	47.67	48.17
Al_2O_3	33.10	33.23	33.20	33.23	33.02	32.67	34.38	33.47	33.45	31.58	32.55	32.71	32.53
MgO	10.38	11.23	10.16	11.33	10.01	11.54	11.70	11.19	10.61	8.39	8.54	8.59	10.24
FeO	5.69	4.04	5.74	3.87	5.60	3.09	2.80	4.01	4.94	8.47	7.97	8.47	5.52
MnO	0.06	0.07	0.05	0.02	0.03	0.05	0.07	0.04	0.11	0.06	0.05	0.04	0.02
CaO	b.d.	b.d.	b.d.	b.d.	b.d.	b.d.	0.01	b.d.	b.d.	b.d.	b.d.	b.d.	0.02
K_2O	0.02	0.02	0.02	0.02	0.02	0.01	0.01	0.01	0.03	0.03	0.03	0.03	0.03
Na_2O	0.08	0.11	0.08	0.16	0.16	0.20	0.30	0.03	0.08	0.11	0.11	0.11	0.32
Total	97.73	98.10	97.95	97.63	97.33	96.03	97.93	97.55	97.78	95.30	97.24	97.62	96.85
H_2O	0.80	0.85	0.72	0.87	0.96	1.04	1.05	1.05	0.60	0.57	0.56	0.61	0.93
CO_2	1.11	1.18	0.88	1.05	1.16	1.61	0.89	1.67	1.31	1.07	1.37	0.68	0.53
Total	99.64	100.13	99.55	99.55	99.45	98.68	99.87	100.27	99.69	96.94	99.17	98.91	98.31
Si	4.962	5.000	4.976	4.982	4.985	4.994	4.914	4.966	4.957	4.972	4.991	4.954	4.980
Al	3.996	3.964	3.998	3.981	3.999	3.966	4.091	4.014	4.023	3.966	3.990	4.006	3.964
Mg	1.585	1.694	1.548	1.717	1.533	1.772	1.761	1.698	1.613	1.333	1.324	1.331	1.578
Fe	0.487	0.342	0.491	0.329	0.481	0.266	0.236	0.341	0.421	0.755	0.693	0.736	0.477
Mn	0.005	0.006	0.004	0.002	0.002	0.004	0.006	0.003	0.009	0.006	0.004	0.004	0.002
Ca	b.d.	b.d.	b.d.	b.d.	b.d.	b.d.	0.002	b.d.	b.d.	b.d.	b.d.	b.d.	0.003
K	0.002	0.003	0.002	0.002	0.002	0.002	0.002	0.002	0.004	0.004	0.004	0.004	0.004
Na	0.016	0.021	0.015	0.032	0.033	0.041	0.059	0.007	0.017	0.023	0.021	0.022	0.064

Note: Chemical formulas normalized to 18 oxygens. b.d. = elements analyzed for, but below detection limits.

* Fine graphite is probably in the cordierite.

** BeO = 0.047, Li_2O = 0.021 (Grew et al., 1987).

† Be < 0.001% (emission spectra, G. R. Rossman, personal communication).

†† Be = 0.0015% (emission spectra, G. R. Rossman, personal communication).

‡ Li = 0.0015 wt%, BeO = 0.002 wt%, B_2O_3 = 0.005 wt% (ion microprobe, E. S. Grew, personal communication).

§ Uneven IR spectral baseline in H_2O stretching region, IR H_2O determinations uncertain.

is much less than the CO_2 contents in many natural cordierites (values up to 2.2 wt% CO_2, Armbruster et al., 1982).

Johannes and Schreyer (1981) postulated that trace amounts of K in the channels of cordierite B might hinder incorporation of the large CO_2 molecules, thus producing the lower CO_2 contents observed for this sample material. Such an interpretation suggests the possibility that the process of volatile equilibration was significantly slower in cordierite B than in cordierite A. This is also supported by the report that decreasing the grain size of cordierite B seemed to lead to the incorporation of higher amounts of CO_2. The data obtained for cordierite A might therefore represent a closer approximation to volatile equilibrium. The results for cordierite A at 5 kbar and 600 °C show maximum CO_2 contents of between 1.5 and 2.0 wt% at $X_{CO_2}^{fluid} = 1.0$ and also more closely resemble the experimental results of Armbruster and Bloss (1980, 1982).

The question of whether the volatile compositions of natural cordierites most closely resemble the experimental results obtained for cordierite A or for cordierite B can be examined by studying natural cordierite samples collected from localities where the peak metamorphic pressures and temperatures have been carefully constrained. Experiments at high P and T have shown that increases in temperature cause the total volatile contents in cordierite to decrease, whereas increases in fluid pressure produce higher total volatile contents (see Figs. 10a, 10b). High-CO_2 natural cordierites have been collected from several localities where the peak metamorphic pressures and temperatures have been carefully constrained. In the present study, cordierite sample 3, from the Pikwitonei granulite domain, Manitoba, Canada (peak metamorphism at 775 °C and 6.1–6.8 kbar; K. Mezger, personal communication), contains 1.97 wt% CO_2. Sample 14, from the Wind River Range, Wyoming (peak metamorphism at >750 °C and 5 kbar; R. Frost, personal communication) contains 1.67 wt% CO_2. Values of up to 1.42 wt% CO_2, and possibly of up to 2.29 wt% CO_2, have been reported for the cordierites from West Uusimaa, Finland (peak metamorphism at 800 °C, 5 kbar; Schreurs, 1985). The CO_2 contents of these natural cordierite samples, collected from metamorphic rocks that reflect relatively high peak metamorphic temperatures at fairly low pressures, are noticeably higher than the experimental data at 600 °C and 5 kbar CO_2 for cordierite B. Most natural cordierites from high-grade metamorphic rocks contain very little K, and the data available strongly suggest that the high CO_2 contents of natural, K-poor samples should not be modeled by using the experimental results for cordierite B.

By verifying that the data for many natural cordierites correspond more closely to the experimental results for cordierite A than for cordierite B, it becomes possible to model the effects of P, T, and $X_{CO_2}^{grd}$ on total channel occupancy and to evaluate the applicability of cordierite for high-grade metamorphic-fluid studies.

Equilibrium volatile contents in the cordierite-H_2O-CO_2 system

Cordierites that are CO_2-rich have lower total volatile contents than H_2O-rich cordierites, and, in metamorphic studies, cordierite equilibria cannot be modeled by using

TABLE 3—*Continued*

20	21**	22	23	24†	25†	26††	27	28	29	31	32	33‡
47.80	48.53	48.90	48.56	48.00	48.73	48.27	49.70	49.40	48.11	48.92	48.95	48.44
32.42	33.03	32.70	33.39	31.91	32.83	32.46	33.75	33.51	32.99	33.45	33.30	33.66
9.20	11.65	11.84	11.92	10.31	10.66	12.02	12.45	12.62	7.60	12.04	12.15	12.85
7.32	3.49	3.24	2.93	5.60	5.58	2.48	1.03	1.57	9.53	2.73	2.81	1.32
0.05	b.d.	0.02	0.03	0.05	0.21	0.07	0.07	0.01	0.46	0.05	0.05	b.d.
b.d.	b.d.	0.01	b.d.	0.02	b.d.	0.01	b.d.	0.02	0.02	0.04	0.03	b.d.
0.08	0.03	0.03	0.02	0.02	0.02	0.02	0.02	0.03	0.03	0.02	0.05	b.d.
0.08	0.37	0.37	0.37	0.20	0.29	0.34	0.18	0.33	0.12	0.20	0.32	0.12
96.95	97.10	97.11	97.22	96.21	98.32	95.67	97.20	97.49	98.86	97.45	97.65	97.39
0.56	1.79	1.73	1.81	1.73§	1.17	1.50	1.29	1.33	1.24	1.75§	1.47	0.74
0.88	0.28	0.35	0.31	0.82	0.44	1.29	0.62	1.04	0.69	0.40	1.31	1.49
98.39	99.17	99.19	99.34	98.67	99.93	98.48	99.11	99.86	100.79	99.60	100.43	99.62
4.976	4.960	4.991	4.945	5.002	4.968	4.983	5.006	4.980	4.965	4.961	4.961	4.978
3.977	3.979	3.933	4.007	3.919	3.945	3.950	4.005	3.982	4.013	3.998	3.976	3.996
1.428	1.775	1.802	1.810	1.601	1.620	1.851	1.869	1.897	1.169	1.820	1.836	1.928
0.637	0.298	0.276	0.249	0.488	0.476	0.214	0.087	0.132	0.823	0.232	0.238	0.111
0.004	b.d.	0.002	0.003	0.005	0.019	0.006	0.006	0.001	0.041	0.004	0.004	b.d.
b.d.	b.d.	0.001	b.d.	0.002	b.d.	0.002	b.d.	0.002	0.002	0.004	0.003	b.d.
0.010	0.004	0.004	0.002	0.003	0.003	0.002	0.002	0.004	0.004	0.003	0.006	b.d.
0.016	0.073	0.072	0.074	0.041	0.058	0.069	0.036	0.065	0.025	0.039	0.062	0.023

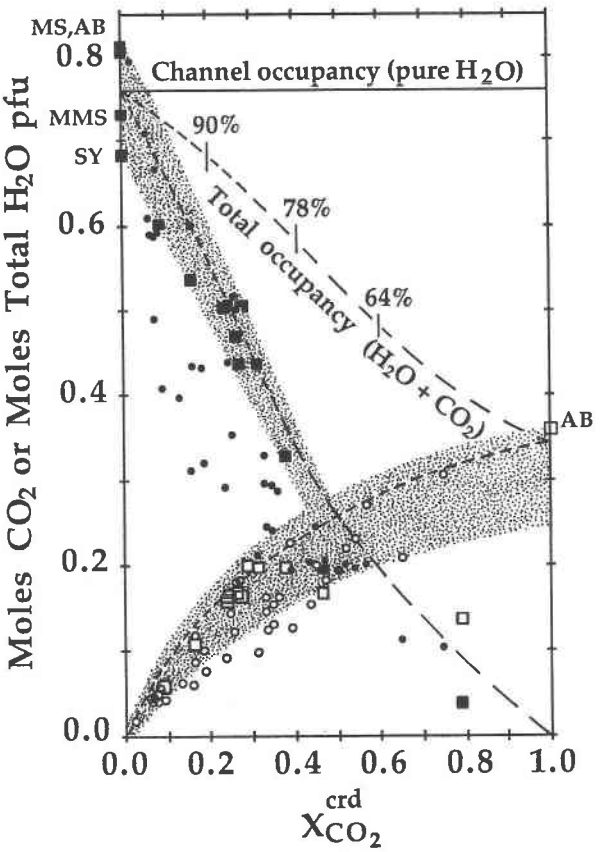

Fig. 11. Comparison of natural cordierite H_2O-CO_2 compositions with results of fluid-saturated experiments at 5 kbar and 600 °C. Natural-sample data (shown by small dots and circles) includes published values for five alkali-rich cordierites (Armbruster and Irouschek, 1983) and one high-CO_2 cordierite (Armbruster et al., 1982). Open symbols indicate CO_2; filled symbols indicate H_2O. Larger square symbols (shaded areas) show experimental data of Johannes and Schreyer (1981, their cordierite A). Experimental data for pure H_2O or pure CO_2 are represented by SY (Schreyer and Yoder, 1964), MMS (Mirwald et al., 1979), MS (Mirwald and Schreyer, 1977), and AB (Armbruster and Bloss, 1982, for which the value shown was interpolated between 4- and 6-kbar data). Upper horizontal solid and upper dashed lines, fit to average experimental data, show channel occupancy by H_2O and effects of CO_2 upon total channel occupancy.

only the data for the pure H_2O system (see upper two lines, Fig. 11). The upper horizontal line in Figure 11 shows the equilibrium volatile content of pure-H_2O cordierite at 600 °C and 5 kbar. The average value depicted is consistent with the range of experimental values obtained in mixed H_2O-CO_2 studies by Johannes and Schreyer (1981). In experiments at the same P and T, Armbruster and Bloss (1980) (AB in Fig. 11) and Mirwald and Schreyer (1977) (MS in Fig. 11) measured total H_2O contents that were approximately 0.5 mol pfu higher; the H_2O contents obtained by Mirwald et al. (1979) (MMS in Fig. 11) and Schreyer and Yoder (1964) (SY in Fig. 11) are about 0.3 mol pfu lower and 0.8 mol pfu lower, respectively. The second dashed curve in Figure 11 shows the effect of CO_2 on total volatile contents in cordierite and is based primarily on the experiments of Johannes and Schreyer (1981) at 600 °C and 5 kbar (shaded). Numbers along this (H_2O + CO_2) curve show total channel occupancies, as a percentage of the pure H_2O value, at different values of $X^{crd}_{CO_2}$. From the data shown, the total equilibrium (H_2O + CO_2) content of a cordierite with $X^{crd}_{CO_2} = 0.2$ will be ~90% of the value for H_2O-saturated cordierite equilibrated at the same P-T conditions. For $X^{crd}_{CO_2} = 0.4$ and 0.60, the total volatile contents are ~78% and 64% of the values for H_2O-saturated cordierite, respectively. If the (H_2O + CO_2) curve is derived instead by using the higher H_2O- and CO_2-content determinations obtained by Mirwald and Schreyer (1977) and Armbruster and Bloss (1980), and by following the uppermost edge of the shaded experimental H_2O and CO_2 data fields in Figure 11, then the total channel occupancy estimates for (H_2O + CO_2) are 95%, 77%, and ~62%, respectively, at $X^{crd}_{CO_2} = 0.2$, 0.4, and 0.6.

Common granulite-facies cordierites contain both H_2O and CO_2, with $X^{crd}_{CO_2}$ usually between 0.3 and 0.7 (Figs. 7, 8). Such samples must have lower total channel occupancies than would be predicted from experiments involving only hydrous cordierite at the appropriate P and T.

We have modeled the effects of P, T, and $X^{crd}_{CO_2}$ on total channel occupancy in cordierite (Fig. 12). This was accomplished by adjusting isopleths of channel occupancy developed for the cordierite-H_2O system (Mirwald and Schreyer, 1977; Armbruster and Bloss, 1980) (Fig. 10a) for the decreases in total channel occupancy that occur as a function of $X^{crd}_{CO_2}$ (Fig. 11). The reductions in total channel occupancy were modeled by applying the experimental results at 5 kbar and 600 °C shown in Figure 11 to all P and T. For example, at $X^{crd}_{CO_2} = 0.4$, total (H_2O + CO_2) contents are modeled to be 78% of the values shown in Figure 10a ($X^{crd}_{CO_2} = 0$). Modeling these reductions in total channel occupancy by using slightly higher H_2O and CO_2 contents, as may be indicated by the results of Mirwald and Schreyer (1977) and Armbruster and Bloss (1980), produces no obvious changes in the isopleth locations for $X^{crd}_{CO_2} > 0.25$. For values of $X^{crd}_{CO_2} < 0.25$, a selection of these higher H_2O and CO_2 data results in somewhat lower estimates for the equilibrium contents of (H_2O + CO_2) at any P and T. The mixed-volatile isopleths can also be derived by using other experimental hydration results, such as those shown in Figure 10b.

It is important to note that the isopleths for H_2O shown in Figure 10a exactly parallel the pressure and temperature increases between the conditions of most experimental studies (5 kbar and 600 °C) and the most commonly reported conditions of granulite-facies metamorphism (7.5 ± 1 kbar and 800 ± 50 °C; Bohlen, 1987). For this reason, it should be possible to apply the experimental data obtained at 5 kbar and 600 °C with some confidence, as a basis for the above extrapolations examining H_2O and CO_2 contents at granulite-facies pressures and temperatures. A similar inspection of the isopleths shown in Figure

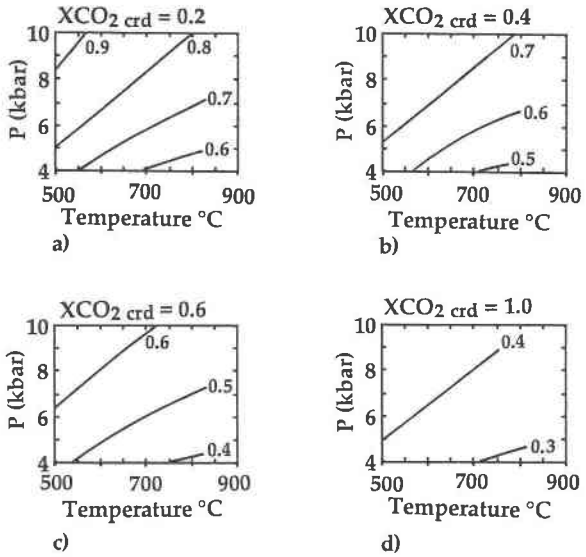

Fig. 12. Effects of P, T, and cordierite X_{CO_2} on total (H_2O + CO_2) occupancy. Cordierites with high X_{CO_2} have lower total volatile contents. Isopleths show total equilibrium volatile contents in moles pfu. Isopleths for the cordierite-H_2O system were taken from Mirwald and Schreyer (1977) and Armbruster and Bloss (1980) (Fig. 10a); isopleths for total volatiles in the mixed H_2O-CO_2 system were modeled from Fig. 10a by using the decreases observed in total volatile contents as a function of cordierite X_{CO_2} at 5 kbar and 600 °C (Fig. 11).

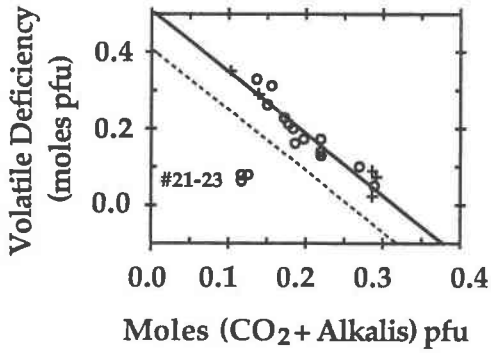

Fig. 13. Volatile deficiency in natural cordierites is inversely related to the amount of (CO_2 + alkalis), which act as "plugs" in the channels. The solid regression line and sample data points indicate volatile deficiencies of natural cordierite samples in comparison to peak metamorphic estimates shown in Fig. 12. The dashed line indicates the linear regression for comparable, slightly smaller volatile deficiency estimates derived on the basis of the isopleths of Helgeson et al. (1978) (Fig. 10b); this dashed line also closely represents estimates based on the isopleths of Mirwald et al. (1979). Data for natural cordierites analyzed in this study are indicated by circles, and data for alkali-rich cordierites (Armbruster and Irouschek, 1983), by crosses. Samples 21–23 may reflect unusual local fluid environments or late high-temperature re-equilibration with H_2O-rich fluids.

10b indicates that slightly lower total volatile contents (~0.1 mol pfu for pure H_2O) could be expected at granulite-facies P-T conditions, compared to the results of experiments at 5 kbar and 600 °C.

Johannes and Schreyer (1981) found that changes in temperature (from 300 to 900 °C) did not affect the partitioning of H_2O and CO_2 between cordierite and a fluid phase. However, they found that increases in pressure produced slightly higher X_{CO_2} values in the cordierite (on the order of $0.02X_{CO_2}$ per kilobar increase in pressure). This effect of pressure was only studied for a narrow range of fluid compositions ($X^{fluid}_{CO_2}$ = 0.61 to 0.70) and only using cordierite B.

Retrograde volatile re-equilibration

When the volatile compositions of natural cordierites are plotted on P, T, $X^{crd}_{CO_2}$ diagrams such as Figure 12, many natural cordierites appear to be relatively volatile deficient. The values of these volatile-deficiency estimates depend strongly upon the accuracies of peak metamorphic pressure and temperature determinations, as well as upon the derivation of Figure 12. Furthermore, because Na-rich cordierites can incorporate more H_2O than Na-poor varieties (Schreyer, personal communication), estimates of volatile deficiency are less well constrained for high-Na samples. Nevertheless, unless the H_2O-CO_2 partitioning between cordierite and a metamorphic-fluid phase changes markedly as a function of pressure from the results of experiments at 5 kbar and 600 °C, the observed volatile deficiencies cannot be correlated to the differences in P and T between the experiments and the peak of metamorphism. Instead, the degree of volatile deficiency is correlated to the content of (CO_2 + alkalis) within the channels (Fig. 13). Both CO_2 and alkali cations have the potential to act as "plugs" in the cordierite channels (Aines and Rossman, 1984), which can retard or prevent volatile re-equilibration.

Only cordierite samples 21–23 have volatile compositions that differ from the trend shown in Figure 13. The hydrous, volatile-rich compositions of these three cordierite samples are anomalous in comparison to all of our other analyses of cordierites from granulite-facies occurrences (see Figs. 7 and 8). Water-rich fluids are uncommon and certainly not pervasive under granulite-facies conditions, where wholesale melting would result. Grew et al. (1987, p. 27) have proposed that the distinctive mineral assemblages of these three cordierite-bearing rocks may reflect an unusual local fluid environment or late high-temperature re-equilibration with H_2O-rich fluids. The remarkably clean and unaltered nature of these three cordierite samples may also support the interpretation of fluid re-equilibration at high temperatures; abundant evidence indicates that cordierite is subject to retrograde breakdown reactions under hydrous conditions at lower pressures and temperatures. Reactions producing "pinite," a mixture of micas, probably occur in cases where K is available in the fluid phase, and an isotropic substance composed of hydrous aluminum silicate is also frequently described. Both the previous petrologic studies by Grew

et al. (1987) and the estimates of cordierite volatile compositions and volatile deficiency obtained in this study support the interpretation that these three samples have retained evidence of unusual metamorphic-fluid conditions.

All of the natural cordierites investigated (except samples 21–23) are indicated to be volatile deficient by 0.05 to 0.35 mol pfu (Fig. 13). Because these low volatile contents are observed in cordierites from a variety of metamorphic environments, rather than only those from the granulite facies, the effect is probably related to volatile losses incurred during uplift and cooling of a metamorphic terrane. The volatile deficiency values calculated for the cordierites in this study did not show a correlation with associated amphibolite- or granulite-facies metamorphic grades. Cordierites that have not lost significant amounts of volatiles, and are thus most suitable for metamorphic-fluid studies, can be readily identified from Figure 13.

The contents of CO_2 and alkali cations in cordierite can be related by using IR absorptivity coefficient ratios for CO_2:$H_2O_{I\text{ or }II}$, in concert with the 2:1 ratio of H_2O_{II} to alkali cations shown in Figure 6. However, because traces of atmospheric CO_2 are difficult to detect in individual IR spectra of cordierite, it is wise to prepare IR working curves.

Preservation of channel-gas compositions

Natural cordierites can be directly used for metamorphic-fluid studies only if channel-gas compositions at peak metamorphic conditions are retained. The question of retrograde volatile re-equilibration in cordierite has been experimentally investigated by Jochum et al. (1983). Their work on hydrous cordierite indicates that in the range of 250–400 °C and 0.5–3 kbar, the isopleths for total channel H_2O swing gently toward negative dP/dT slopes. Cordierites that re-equilibrate fully to surface conditions should therefore be essentially anhydrous. Obviously, volatiles are retained in cordierite at surface conditions, reflecting kinetic barriers to outward fluid movement. Experimental studies of the dehydration kinetics for synthetic hydrous pure-Mg cordierite (Jochum et al., 1983) reveal that outward diffusion of water is generally much slower than inward diffusion into the channels. Experiments at P_{H_2O} = 1 kbar and T = 300 °C suggest that the time of re-equilibration for H_2O in a 2-mm crystal of pure-Mg cordierite lies between about 2 and 200 m.y. (Schreyer, 1985). Natural cordierites, which contain both large CO_2 molecules and alkali cations in the channels, should undergo re-equilibration even more slowly.

C isotopes

C isotopes provide a means to evaluate the extent to which exchange may have modified the CO_2 compositions in natural cordierites (Vry et al., 1988). In some regions, notably in the Pikwitonei granulite domain of the Superior province, Manitoba, Canada, coexisting granulite-facies cordierites and graphites preserve distinctive, low $\delta^{13}C$, sedimentary values. The isotopically light compositions of graphites from pelites and iron formations in the Pikwitonei region ($\delta^{13}C_{gr} = -24.7$ to -44.5, mean -34.9) are comparable to other analyses of carbonaceous matter from lower-grade graphitic shales of the same age in the Superior province (Strauss, 1986). Because no other source of such low C-isotope values is known, these graphites provide a valuable marker for C-isotope studies of coexisting cordierite and graphite. In the Pikwitonei region, four cordierites have $\delta^{13}C_{crd} = -31.8$ to -34.9, coexisting graphites have $\delta^{13}C_{gr} = -36.1$ to -41.8, and the values for the fractionation between cordierite and graphite ($\Delta^{13}C_{crd\text{-}gr}$ = 4.3, 6.6, 7.0, and 7.7) approximate $\Delta^{13}C_{CO_2\text{-}gr}$, which at granulite-facies temperatures is 5.6 to 8.2 (Friedman and O'Neil, 1977; Valley and O'Neil, 1981). Even though volatile losses for these samples are inferred to be quite high (~25% to 35% of original volatile content for sample 1), the $\Delta^{13}C_{crd\text{-}gr}$ values approximate the predicted high-temperature fractionation and show no reversals. Similar fractionations have also been obtained for cordierites from three other amphibolite- or granulite-facies terranes. Values of $\Delta^{13}C_{crd\text{-}gr}$ show no relation to $\delta^{13}C_{gr}$, which varies from -10.5 to -41.8. The isotopic results are consistent with the approximate preservation of peak metamorphic C-isotope compositions in cordierites.

Isotopically light $\delta^{13}C$ values have been obtained for a number of granulite-facies cordierites ($\delta^{13}C_{crd} < -15$) and graphites. These values place severe restrictions on theories of massive CO_2 infiltration ($\delta^{13}C_{fluid} > -7$). Calculated CO_2/rock ratios for samples from several granulite terranes are <0.01 by weight (~0.016 on a molar oxygen basis) (Vry et al., 1988). The isotopic data are consistent with limited amounts of leakage of channel volatiles, but not with extensive exchange, or retrograde re-equilibration with an externally derived CO_2-bearing fluid ($\delta^{13}C_{fluid} > -7$). These results indicate that studies of cordierite volatiles can provide useful information about high-grade metamorphic-fluid conditions, if the effects of retrograde re-equilibration are evaluated.

The available data suggest that cordierites can lose volatiles while approximately preserving peak metamorphic $\delta^{13}C$ values of channel CO_2. It is possible that during uplift, both H_2O and CO_2 are lost, in sequence, from the channels. In this case, retrograde volatile losses would have little effect upon estimates of metamorphic-fluid compositions at peak metamorphic conditions. Alternatively, H_2O might be preferentially lost from the channels, in which case volatile losses will have significant impacts upon estimates of metamorphic-fluid compositions at peak metamorphic conditions. For cordierites having small grain sizes, or fractures or inclusions of other minerals, preferential H_2O loss may be a dominant mechanism. Preferential losses, or gains of water are more difficult to explain for cordierites that are clean, unfractured, and initially CO_2-rich. For many natural cordierite samples, some combination of the above mechanisms may apply. It is possible to evaluate the maximum effects of volatile losses on estimates of metamorphic-fluid compositions by using

the upper line shown in Figure 13 and assuming that only H_2O is lost from the channels. This approach will provide maximum estimates for $X_{CO_2}^{fluid}$.

The volatile contents of natural cordierites should reflect conditions encountered during retrograde uplift and cooling, and for this reason the rarity of cordierite samples that show evidence of volatile gains or of CO_2 exchange with an externally derived fluid phase is surprising. Initially isobaric cooling has been proposed for a number of granulite terranes (summarized in Bohlen, 1987). Figures 10 and 12 show that if a free fluid phase was available during initial isobaric cooling, cordierites in such terranes should gain volatiles. However, none of the samples studied (except samples 21–23) showed evidence of increased volatile contents. This observation might result from any of several possible causes, including (1) lack of a free fluid phase during the initial phases of retrogression; (2) losses of volatiles during retrograde uplift; (3) cordierite breakdown to other minerals, if retrograde metamorphism occurs in the presence of a water-rich fluid phase; and (4) the presence of large CO_2 molecules and cations such as Na, Ca, and K in the channels, which probably function to hinder both retrograde volatile gains and losses. At present there are not sufficient data to evaluate the importance of these different possibilities, but the consistency of the results shown in Figure 13 suggests that the presence of CO_2 and (Na + Ca + K) is important and that the volatile-deficiency estimates derived in this study provide evidence of a common metamorphic process.

Metamorphic-fluid studies

Cordierite participates in a number of reactions sensitive to pressure, temperature, and $X_{CO_2}^{fluid}$. Several studies have proposed that the stability relations of reactions involving cordierite can provide information about metamorphic water fugacities and metamorphic pressures (summarized in Lonker, 1981; Bhattacharya, 1986; and Deer et al., 1986). However, because natural cordierites commonly contain both H_2O and CO_2, it is not possible to directly apply cordierite geobarometers and "water-fugacity indicators" (cf. Holdaway and Lee, 1977; Martignole and Sisi, 1981; Bhattacharya, 1986) based on only experimental data for hydrous cordierite. Volatile contents of CO_2-rich cordierites are much lower than those of H_2O-rich cordierites at the same P and T conditions (Figs. 11, 12). Furthermore, natural cordierites may have suffered volatile losses after the peak of metamorphism. As a result, the "water-fugacity indicators" do *not* strictly monitor H_2O fugacities in a fluid phase; instead, for any given $X_{CO_2}^{crd}$, these indicators will give only a lower limit of total fluid (H_2O + CO_2). The derived fugacity determinations are subject to such large uncertainties (on the order of several kilobars, for volatile losses of 0.1 to 0.2 mol pfu) that the estimates will be of questionable value for metamorphic studies.

Estimates of metamorphic-fluid compositions ($X_{CO_2}^{fluid}$) for many granulite-facies cordierites are affected less by volatile losses than are the derived fugacity determinations. If cordierites are assumed to have retained volatile contents from peak metamorphic conditions, or if retrograde volatile losses affect H_2O and CO_2 equally, then the experimental results of Johannes and Schreyer (1981, their Fig. 4A, cordierite A) can be used to estimate corresponding peak metamorphic $X_{CO_2}^{fluid}$ values. Although these experimental data are strictly applicable only at 5 kbar and 600 °C, they should also provide a useful indication of metamorphic-fluid compositions at the commonly reported conditions of granulite-facies metamorphism (7.5 ± 1 kbar and 800 ± 50 °C; Bohlen, 1987). If, instead, cordierites are assumed to be subject to preferential losses of H_2O during retrogression, the maximum effects of volatile losses on estimates of metamorphic-fluid compositions can be evaluated by assuming that only H_2O is lost from the channels. This assumption provides maximum values for $X_{CO_2}^{fluid}$. Retrograde volatile losses can occur if the metamorphic uplift path falls below the isopleths of total volatile content in cordierite (Fig. 12) and if the cordierites are poor in CO_2 and alkalis (Fig. 13).

Without any correction for retrograde volatile losses, the high $X_{CO_2}^{crd}$ values observed for many natural granulite-facies cordierites in this study ($X_{CO_2}^{crd} > 0.3$, see Fig. 7) would imply fluid compositions with $X_{CO_2}^{fluid}$ generally >0.7 (Johannes and Schreyer, 1981, their Fig. 4A). If the observed channel-gas compositions reflect preferential losses on the order of 0.2 mol H_2O pfu (see Fig. 13), fluid composition estimates for these same granulite-facies samples drop significantly, but $X_{CO_2}^{fluid}$ values are still indicated to be greater than $\gtrsim 0.54$.

The use of $X_{CO_2}^{crd}$ values to provide metamorphic-fluid ($X_{CO_2}^{fluid}$) estimates presupposes the existence of a fluid phase during high-grade metamorphism. The question of whether a free fluid phase exists in the deep crust is, however, controversial, and it is certain that fluid regimes in the deep crust are complex (Valley et al., 1983, 1990).

Discussion

Implications for granulite genesis

Two major disparate models currently exist to explain the low water activities characteristic of granulite terranes. Classically, low a_{H_2O} has been attributed to magmatic processes, in particular to water absorption by magmas, which can cause fluid-absent conditions or concentrate CO_2 in the small amounts of residual fluid (Fyfe, 1973a, 1973b; Lamb and Valley, 1984, 1985; Valley and O'Neil, 1984; Valley, 1985; Cartwright and Barnicoat, 1987; Lamb et al., 1987; Waters, 1988; Valley et al., 1990). Low values of a_{H_2O} have also been proposed to result from the pervasive infiltration of large amounts of CO_2 from depth (Janardhan et al., 1979; Newton et al., 1980; Friend, 1983; Glassley, 1983a, 1983b; Touret and Dietvorst, 1983; Newton, 1986).

Most of the granulite-facies cordierites in this study are characterized (Figs. 7 and 8) by a combination of low total

volatile contents, high but variable X_{CO_2} (generally $X^{crd}_{CO_2} = 0.3$ to 0.7), and extremely low contents of channel alkalis [(Na + K + Ca) $\leq$ 0.05 mol pfu]. The high $X^{crd}_{CO_2}$ values result largely from low total H_2O (Fig. 8). Many of these samples, however, appear to be volatile-deficient by 0.1 to 0.2 mol pfu (Fig. 13). If retrograde volatile losses do not alter the proportions of H_2O to CO_2 in the cordierite channels, these high $X^{crd}_{CO_2}$ values indicate metamorphic-fluid compositions at peak metamorphic conditions with $X^{fluid}_{CO_2}$ generally >0.7 (Johannes and Schreyer, 1981, Fig. 4A). If the observed channel-gas compositions reflect preferential losses of H_2O on the order of 0.2 mol pfu (see Fig. 12), then the $X^{fluid}_{CO_2}$ estimates for these same granulite-facies samples may be somewhat lower. The inferred metamorphic-fluid compositions are, however, still CO_2-dominated, with minimum $X^{fluid}_{CO_2}$ values $\gtrsim$0.54 for most granulite-facies samples in this study. It is important to note that such estimates of $X^{fluid}_{CO_2}$ do not reliably reflect fluid saturation or quantities of fluid.

C-isotope studies of coexisting granulite-facies cordierites and graphites indicate that $\delta^{13}C$ values for channel CO_2 in cordierite are not greatly altered after the peak of metamorphism (Vry et al., 1988). The presence of isotopically light C in granulite-facies cordierites ($\delta^{13}C_{crd} < -15$) and graphites is consistent with the possibility of some leakage of channel volatiles, but not with either extensive exchange or retrograde re-equilibration with an externally derived CO_2-bearing fluid ($\delta^{13}C_{fluid} > -7$); thus the isotopically light C severely restricts theories of massive CO_2 infiltration ($\delta^{13}C_{fluid} > -7$). The CO_2/rock ratios for samples from a number of granulite terranes are estimated to be <0.01 by weight (~0.016 on a molar oxygen basis) (Vry et al., 1988). These isotopic data emphasize the importance of local fluid buffering in the granulite facies. Processes of partial melting enrich CO_2 in residual fluids and can lead to conditions of fluid-absent metamorphism. However, the verification of fluid-absent or fluid-present metamorphic conditions using $P(H_2O + CO_2)$ estimates from volatile compositions in cordierite is not practical, because serious errors are introduced if volatile losses have occurred and because CO_2 is present. It is likely that the fluid regime in the deep crust is complex and that different processes can predominate on a local scale.

Acknowledgments

The authors wish to thank T. Chacko, M. Cosca, R. Frost, E. Grew, K. Mezger, D. Moecher, and D. Perkins for providing cordierite samples used in this study, and especially Th. Armbruster for providing both cordierite samples and corresponding analytical data. R. Hervig at Arizona State University, S. R. Dunn, Mount Holyoke College, and J. R. O'Neil at the U.S. Geological Survey at Menlo Park provided H_2O analyses of cordierite samples. K. Mezger, University of Michigan–Ann Arbor, provided *P-T* determinations for rocks from the Pikwitonei domain, Manitoba, and W. Weber at the Manitoba Geological Survey provided support for our work in the Pikwitonei region. M. Sanders and E. Glover at the University of Wisconsin–Madison, and J. Morrison, University of Southern California, were most helpful in providing, respectively, assistance with the IR equipment, with the electron microprobe, and with stable-isotope techniques. Th. Armbruster, T. Chacko, G. Rossman, and W. Schreyer reviewed the preliminary draft of the paper and provided many interesting and helpful comments. Some figures were drafted by P. Dombrowski. This work has been supported in part by grants from Gas Research Institute, 5086-260-1425 (J.W.V.); the National Science Foundation, EAR85-08102 and EAR88-05470 (J.W.V. and P.E.B.); the Petroleum Research Fund, 18839-AC2 (J.W.V.); and NASA, NAG9-189 (P.E.B.).

References cited

Aines, R.D., and Rossman, G. (1984) The high temperature behavior of water and carbon dioxide in cordierite and beryl. American Mineralogist, 69, 319–327.

Armbruster, Th. (1986) Role of Na in the structure of low cordierite: A single crystal X-ray study. American Mineralogist, 71, 746–757.

Armbruster, Th., and Bloss, F.D. (1980) Channel CO_2 in cordierites. Nature, 286, 140–141.

——— (1982) Orientation and effects of channel H_2O and CO_2 in cordierite. American Mineralogist, 67, 284-291.

Armbruster, Th., and Irouschek, A. (1983) Cordierites from the Lepontine Alps: Na + Be → Al substitution, gas content, cell parameters and optics. Contributions to Mineralogy and Petrology, 82, 389–396.

Armbruster, Th., Schreyer, W., and Hoefs, J. (1982) Very high CO_2 cordierite from Norwegian Lapland: Mineralogy, petrology, and carbon isotopes. Contributions to Mineralogy and Petrology, 81, 262–267.

Beltrame, R.J., Norman, D.E., Alexander, E.C., and Sawkins, F.J. (1976) Volatiles released by step-heating a cordierite to 1200 °C. EOS, 57, 352.

Bence, A.E., and Albee, A.L. (1968) Empirical correction factors for the electron microanalysis of silicates and oxides. Journal of Geology, 76, 382–403.

Bhattacharya, A. (1986) Some geobarometers involving cordierite in the FeO-Al_2O_3-SiO_2 (±H_2O) system: Refinements, thermodynamic calibration, and applicability in granulite facies rocks. Contributions to Mineralogy and Petrology, 94, 387–394.

Bohlen, S.R. (1987) Pressure-temperature-time paths and a tectonic model for the evolution of granulites. Journal of Geology, 95, 617–632.

Carson, D.G., Rossman, G.R., and Vaughan, R.W. (1982) Orientation and motion of water molecules in cordierite: A proton nuclear magnetic resonance study. Physics and Chemistry of Minerals, 8, 14–19.

Cartwright, I., and Barnicoat, A.C. (1987) Petrology of Scourian supracrustal rocks and orthogneisses from Stoer, N.W. Scotland: Implications for the geological evolution of the Lewisian complex. In R.G. Park and J. Tarney, Eds., Evolution of the Lewisian and comparable Precambrian high grade terrains. Geological Society Special Publication 27, 93–107.

Chacko, T., Ravinda Kumar, G.R., and Newton, R.C. (1987) Metamorphic *P-T* conditions of the Kerala (South India) khondalite belt, a granulite-facies supracrustal terrain. Journal of Geology, 95, 343–358.

Cohen, J. P., Ross, F.K., and Gibbs, G.V. (1977) An X-ray and neutron diffraction study of hydrous low cordierite. American Mineralogist, 62, 67–78.

Damon, P.E., and Kulp, J.L. (1958) Excess helium and argon in beryl and other minerals. American Mineralogist, 43, 433–459.

Deer, W.A., Howie, R.A., and Zussman, J. (1986) Rock-forming minerals, vol. 1B: Disilicates and ring silicates (2nd edition), p. 410–540. Wiley, New York.

Duncan, J.F., and Johnston, J.H. (1974) Single-crystal ^{57}Fe Mössbauer studies of the site positions in cordierite. Australian Journal of Chemistry, 27, 249–258.

Farmer, V.C., Ed. (1974) The infrared spectra of minerals, 539 p. Mineralogical Society, London.

Farrell, F., and Newnham, R.E. (1967) Electronic and vibrational absorption spectra in cordierite. American Mineralogist, 52, 380–388.

Friedman, I., and O'Neil, J.R. (1977) Data of geochemistry. U.S. Geological Survey Professional Paper 440-KK.

Friend, C.R.L. (1983) The link between charnockite formation and granite production: Evidence from Kabbaldurga, Karnataka, southern India. In M.P. Atherton and C.D. Gribble, Eds., Migmatites, melting and metamorphism, p. 264–276. Shiva Publishing Ltd., Nantwich, Cheshire, U.K.

Fyfe, W.S. (1973a) The granulite facies, partial melting and the Archean

crust. Philosophical Transactions of the Royal Society of London, A. Mathematical and Physical Sciences, 273, 457–461.

——— (1973b) The generation of batholiths. Tectonophysics, 17, 273–283.

Gibbs, G.V. (1966) The polymorphism of cordierite I: The crystal structure of low cordierite. American Mineralogist, 51, 1068–1087.

Glassley, W.E. (1983a) Deep crustal carbonates as CO_2 fluid sources: Evidence from metasomatic reaction zones. Contributions to Mineralogy and Petrology, 84, 14–24.

——— (1983b) The role of CO_2 in the chemical modification of deep continental crust. Geochimica et Cosmochimica Acta, 47, 597–616.

Goldman, D.S., Rossman, G.R., and Dollase, W.A. (1977) Channel constituents in cordierite. American Mineralogist, 62, 1144–1157.

Gordillo, C.E., Schreyer, W., Werding, G., and Abraham, K. (1985) Lithium in Na,Be-cordierites from El Peñón, Sierre de Córdoba, Argentina. Contributions to Mineralogy and Petrology, 90, 93–101.

Grew, E.S. (1986) Petrogenesis of kornerupine at Waldheim (Sachsen), German Democratic Republic. Zeitschrift für geologishe Wissenschaften, 14, 525–558.

Grew, E.S., Abraham, K., and Medenbach, O. (1987) Ti-poor hoegbomite in kornerupine-cordierite-sillimanite rocks from Ellammankovilpatti, Tamil Nadu, India. Contributions to Mineralogy and Petrology, 95, 21–31.

Gunter, A.E. (1977) Water in synthetic cordierites and its significance in the experimental reaction aluminous biotite + sillimanite + quartz = iron cordierite + sanidine + water. Geological Association of Canada Program with Abstracts, 2, 22.

Hawthorne, F.C., and Černý, P. (1977) The alkali metal positions in Cs-Li beryl. Canadian Mineralogist, 15, 412–421.

Helgeson, H.C., Delany, J.M., Nesbitt, H.W., and Bird, D.K. (1978) Summary and critique of the thermodynamic properties of rock-forming minerals. American Journal of Science, 278A, 1–229.

Hochella, M.F., Jr., Brown, G.E., Jr., Ross, F.K., and Gibbs, G.V. (1979) High-temperature crystal chemistry of hydrous Mg- and Fe-cordierites. American Mineralogist, 64, 337–351.

Holdaway, M.J., and Lee, S.M. (1977) Fe-Mg cordierite stability in high-grade pelitic rocks based on experimental theoretical and natural observations. Contributions to Mineralogy and Petrology, 63, 175–198.

Hörmann, P.K., Raith, M., Raase, P., Ackermand, D., and Seifert, F. (1980) The granulite complex of Finnish Lapland: Petrology and metamorphic conditions in the Ivaljoki-Inarijärvi area. Geological Survey of Finland Bulletin, 308, 1–95.

Iiyama, T. (1960) Recherches sur le rôle de l'eau dans la structure et le polymorphisme de la cordiérite. Bulletin de la Société française de Minéralogie et de Cristallographie, 83, 155–179.

Janardhan, A.S., Newton, R.C., and Smith, J.V. (1979) Ancient crustal metamorphism at low P_{H_2O}: Charnockite formation at Kabbaldurga, south India. Nature, 278, 511–514.

Jochum, C., Mirwald, P.W., Maresch, W., and Schreyer, W. (1983) The kinetics of H_2O exchange between cordierite and fluid during retrogression. Fortschritte der Mineralogie, 61, no. 1, 103–105.

Johannes, W., and Schreyer, W. (1977) Verteilung von H_2O und CO_2 zwischen Mg-cordierit und fluider phase. Fortschritte der Mineralogie, 55, no. 1, 64–65.

——— (1981) Experimental introduction of CO_2 and H_2O into Mg-cordierite. American Journal of Science, 281, 299–317.

Kitsul, V.I., Lasebnik, Yu.D., Brovkin, A.A., Suknev, V.S., Kulagina, D.A., and Burakov, A.A. (1971) Methods and results of study of cordierites of the granulite facies. In V.I. Kitsul, Ed., Petrologiya Granulitovoi Fatsii Aldanskogo Shchita, p. 114–123. Nauka, Moscow.

Lamb, W.M., and Valley, J.W. (1984) Metamorphism of reduced granulites in low-CO_2 vapour-free environment. Nature, 312, 56–58.

——— (1985) C-O-H fluid calculations and granulite genesis. In A.C. Tobi and J.L.R. Touret, Eds., The deep Proterozoic crust in the North Atlantic provinces, p. 119–131. Reidel, Dordrecht, Netherlands.

Lamb, W.M., Valley, J.W., and Brown, P.E. (1987) Post-metamorphic CO_2-rich fluid inclusions in granulites. Contributions to Mineralogy and Petrology, 96, 485–495.

Lepezin, G.G., Kuznetsova, I.K., Lavrenten'ev, Yu.G., and Chmel'nicova, O.S. (1976) Optical methods of determination of the water contents in cordierites. Contributions to Mineralogy and Petrology, 58, 319–329.

Lonker, S.W. (1981) The *P-T-X* relations of the cordierite-garnet-sillimanite-quartz equilibrium. American Journal of Science, 63, 1056–1090.

Martignole, J., and Sisi, J.C. (1981) Cordierite-garnet-H_2O equilibrium: A geological thermometer, barometer, and water fugacity indicator. Contributions to Mineralogy and Petrology, 77, 38–46.

Meagher, E.P. (1967) The crystal structure and polymorphism of cordierite. Ph.D. thesis, Pennsylvania State University, University Park.

Medenbach, O., Maresch, W.V., Mirwald, P.W., and Schreyer, W. (1979) Optische Bestimmung des H_2O-Gehalts synthetischer Mg-Cordierite. Fortschritte der Mineralogie, 57, Beiheft 1, 99–101.

Medenbach, O., Maresch, W.V., Mirwald, P.W., and Schreyer, W. (1980) Variation of refractive index in synthetic Mg-cordierite with H_2O. American Mineralogist, 65, 367–373.

Mirwald, P.W., and Schreyer, W. (1977) Die stabile und metastabile Abbaureaktion von Mg-Cordierit in Talk, Disthen und Quarz und ihre Abhängigkeit vom Gleichgewichtswassergehalt des Cordierits. Fortschritte der Mineralogie, 55, 95–97.

Mirwald, P.W., Maresch, W.V., and Schreyer, W. (1979) Der Wassergehalt von Mg-Cordierit zwischen 500 ° und 800 °C sowie 0.5 und 11 kbar. Fortschritte der Mineralogie, 57, Beiheft 1, 101–102.

Mottana, A.R., Fusi, A., Potenza, B.B., Crespi, R., and Liborio, G. (1983) Hydrocarbon-bearing cordierite from the Dervio-Colico road tunnel (Como, Italy). Neues Jahrbuch für Mineralogie, Abhandlungen, 148, 188–199.

Newton, R.C. (1986) Fluids of granulite facies metamorphism. In J.V. Walther, and B.J. Wood, Eds., Fluid-rock interactions during metamorphism, p. 36–59. Springer, New York.

Newton, R.C., Smith, J.V., and Windley, B.F. (1980) Carbonic metamorphism, granulites, and crustal growth. Nature, 288, 45–50.

Norman, D.I., Alexander, E.C., Jr., and Sawkins, F.J. (1976) Helium in cordierites: A possible indicator of low temperature metamorphic events (abs.). EOS, 57, 352.

Perreault, S., and Martignole, J. (1986) CO_2-rich cordierites in high-temperature migmatites, north-eastern Grenville province, Quebec (abs.). Geological Association of Canada Program with Abstracts, 11, 114.

Peterson, D.E., and Valley, J.W. (1988) Comparison of ideal and non-ideal orthopyroxene activities in Alm-Fs and Pyr-En geobarometry (abs.). Geological Society of America Abstracts with Programs, 20, A98.

Povondra, P., and Langer, K. (1971) Synthesis and some properties of sodium-beryllium bearing cordierite, $Na_xMg_2(Al_{4-x}Be_xSi_5O_{18})$. Neues Jahrbuch für Mineralogie, Abhandlungen, 116, 1–19.

Pryce, M.W. (1973) Low-iron cordierite in phlogopite schist from White Well, Western Australia. Mineralogical Magazine, 39, 241–243.

Robinson, P., Tracy, R.J., Hollocher, K.T., Schumacher, J.C., and Henry, N.B., IV. (1986) The central Massachusetts metamorphic high. In P. Robinson, Ed., Regional metamorphism and metamorphic phase relations in north-western and central New England, p. 195–284. University of Massachusetts Amherst Contributions 59.

Schreurs, J. (1985) The west Uusimaa low pressure thermal dome, S.W. Finland, 178 p. Rodopi, Amsterdam.

Schreyer, W. (1985) Experimental studies on cation substitutions and fluid incorporation in cordierite. Bulletin de la Société française de Minéralogie et de Cristallographie, 108, 273–291.

Schreyer, W., and Yoder, H.S. (1964) The system Mg-cordierite and related rocks. Neues Jahrbuch für Mineralogie, Abhandlungen, 101, 271–342.

Selkregg, K., and Bloss, F.D. (1980) Cordierites: Compositional controls of Δ, cell parameters, and optical properties. American Mineralogist, 65, 522–533.

Strauss, H. (1986) Carbon and sulfur isotopes in Precambrian sediments from the Canadian Shield. Geochimica et Cosmochimica Acta, 50, 2653–2662.

Suknev, V.S., Kitsul, V.I., Lazebnik, Yu.D., and Brovkin, A.A. (1971) Quantitative determination of CO_2 in cordierites by infrared spectroscopy and chemical analysis. Doklady Akademii Nauk SSSR, 200, 156–158.

Touret, J., and Dietvorst, P. (1983) Fluid inclusions in high-grade anatectic metamorphites. Journal of the Geological Society of London, 140, 635–649.

Valley, J.W. (1985) Polymetamorphism in the Adirondacks: Wollastonite at contacts of shallowly intruded anorthosite. In A.C. Tobi and J.L.R.

Touret, Eds., The deep Proterozoic crust in the North Atlantic provinces, p. 217–236. Reidel, Dordrecht, Netherlands.

Valley, J.W., and O'Neil, J.R. (1981) $^{13}C/^{12}C$ exchange between calcite and graphite: A possible thermometer in Grenville marbles. Geochimica et Cosmochimica Acta, 45, 411–419.

——— (1984) Fluid heterogeneity during granulite facies metamorphism in the Adirondacks: Stable isotope evidence. Contributions to Mineralogy and Petrology, 85, 158–173.

Valley, J.W., McLelland, J., Essene, E.J., and Lamb, W.M. (1983) Metamorphic fluids in the deep crust: Evidence from the Adirondack Mountains, N.Y. Nature, 301, 226–228.

Valley, J.W., Bohlen, S.R., Essene, E.J., and Lamb, W.M. (1990) Metamorphism in the Adirondacks. II. The role of fluids. Journal of Petrology, in press.

Vry, J.K., Brown, P.E., Valley, J.W., and Morrison, J. (1988) Constraints on granulite genesis from carbon isotopic compositions of cordierite and graphite. Nature, 332, 66–68.

Wallace, J.H., and Wenk, H.R. (1980) Structure variation in low cordierites. American Mineralogist, 65, 96–111.

Waters, D.J. (1988) Partial melting and the formation of granulite facies assemblages in Namaqualand, South Africa. Journal of Metamorphic Geology, 6, 387–404.

Wood, D.L., and Nassau, K. (1967) Infrared spectra of foreign molecules in beryl. Journal of Chemical Physics, 47, 2220–2228.

Zimmerman, J.L. (1981) The liberation of H_2O, CO_2, and hydrocarbons from cordierites: Kinetics, structural sites, and petrogenetic implications. Bulletin de la Société française de Minéralogie et de Cristallographie, 104, 325–338.

Manuscript received January 17, 1989
Manuscript accepted September 25, 1989